



Cellular correlates of compensatory axonal sprouting in the magnocellular neurosecretory system of the rat

by John Andrew Watt

A thesis submitted in partial fulfillment of the requirements for the degree of Doctor of Philosophy in Biological Sciences

Montana State University

© Copyright by John Andrew Watt (1993)

Abstract:

Neuronal and non-neuronal correlates of compensatory sprouting in the neural lobe (NL) were investigated using a unilateral hypothalamic knife-cut of the hypothalamoneurohypophysial tract to partially denervate the rat NL. Metabolic, morphometric and immunocytochemical methods were employed to investigate the cellular activity which accompanies the magnocellular neurosecretory system's response to partial denervation. Analysis of the metabolic effects of partial denervation indicate a transient urine hypoosmolality within the first 24 hours post-surgery (PS) followed by a chronic urine hyperosmolality which persists throughout the 3 month investigative period. Daily water intake (drinking) and urine excretion volumes demonstrate drop below control levels immediately following surgery which persists throughout the investigative period. Morphometric measurement of the magnocellular oxytocinergic and vasopressinergic neurons in the contralateral supraoptic nucleus (SON) demonstrated an enlargement of both cell populations within 10 days PS which remained significantly above control levels for at least 30 days PS. These data also suggest the oxytocinergic cell population may enlarge more vigorously or at an earlier time than their vasopressinergic counterparts. Cell counts of glial cell nuclei within 1 micron coronal sections of the NL revealed an increase in the number of pituicyte nuclei by 2 days PS which remained above age-matched control values for at least 30 days PS. The number of microglial cell nuclei numbers increased by 2 days PS but returned to normal by 10 days PS. Morphometric analysis of the NL vascular plexis revealed a strong temporal correlation between the enlargement of the NL vascular plexis and the process of compensatory collateral sprouting of neurosecretory axons in the NL. Immunocytochemical analysis of bromodeoxyuridine (BrdU) substitution suggests that the microglial but not the pituicyte populations within the NL are undergoing hyperplasia between 1 and 6 days following partial denervation. Analysis of nerve growth factor receptor (NGFR) expression in the NL indicates a dramatic increase in the proportional area immunoreactive for NGFR between 5 and 10 days PS, which then returns to normal levels. Immunocytochemical comparison between NGFR, iC3b complement receptor and leukocyte common antigen (LCA) immunoreactivity suggest that a subpopulation of microglial cells may up-regulate their expression and/or increase the numbers of cells expressing the NGF receptor during a period when axonal degeneration and phagocytosis of neuronal debris is occurring. These data describe the varieties of neuronal and non-neuronal activities which underlie the compensatory axonal sprouting of intact magnocellular neurons within the partially denervated NL.

CELLULAR CORRELATES OF COMPENSATORY AXONAL SPROUTING  
IN THE MAGNOCELLULAR NEUROSECRETORY SYSTEM  
OF THE RAT

by

John Andrew Watt

A thesis submitted in partial fulfillment  
of the requirements for the degree

of

Doctor of Philosophy

in

Biological Sciences

MONTANA STATE UNIVERSITY  
Bozeman, Montana

January 1993

D378  
W34

APPROVAL

of a thesis submitted by

John Andrew Watt

This thesis has been read by each member of the thesis committee and has been found to be satisfactory regarding content, English usage, format, citations, bibliographic style, and consistency, and is ready for submission to the College of Graduate Studies.

Jan. 13, 1993  
Date

Charles M. Paden  
Chairperson, Graduate Committee

Approved for the Major Department

14 January 1993  
Date

Robert S. Moore  
Head, Biology Department

Approved for the College of Graduate Studies

1/15/93  
Date

R. L. Brown  
Graduate Dean

## STATEMENT OF PERMISSION TO USE

In presenting this thesis in partial fulfillment of the requirements for a doctoral degree at Montana State University, I agree that the Library shall make it available to borrowers under rules of the Library. I further agree that copying of this thesis is allowable only for scholarly purposes, consistent with "fair use" as prescribed in the U.S. Copyright Law. Requests for extensive copying or reproduction of this thesis should be referred to University Microfilms International, 300 North Zeeb Road, Ann Arbor, Michigan 48106, to whom I have granted "the exclusive right to reproduce and distribute copies of the dissertation in and from microfilm and the right to reproduce by abstract in any format."

Signature

Date

*John Andrew Watt*  
*January 13, 1993*

## TABLE OF CONTENTS

INTRODUCTION.....	1
Statement of Purpose.....	1
Plasticity in the Mammalian Central Nervous System.....	3
The Magnocellular Neurosecretory System.....	5
The Fine Structure of the Neural Lobe.....	7
Development of the Vascular Plexus of the Neurohypophysis.....	9
Neuronal Reorganization and Recovery of Function.....	12
Sprouting in the Magnocellular and Parvocellular Neurosecretory Systems.....	14
Nerve Growth Factor and its Receptors.....	19
Justification, Rational and Specific Objectives.....	23
Role of Glia in Axonal Sprouting.....	23
Neuronal Activation in Axonal Sprouting.....	26
Specific Objectives.....	28
Non-neuronal Response to Injury.....	28
Neuronal Activity.....	29
METHODS.....	30
Animals.....	30
Surgery.....	30
Tissue Preparation.....	31
Tissue Microtomy.....	33
Immunohistochemistry.....	33
Image Analysis and Morphometric Measurements.....	38
192-IgG Proportional Area Analysis.....	38
SON Cellular Morphometry.....	39
Glial Morphometry.....	40
Metabolic Analysis.....	41
Statistical Analysis.....	41
RESULTS.....	42
Post-Mortem Observations Within the Hypothalamus.....	42
Lesion-Induced Changes in Urine Osmolality, Excretion and Daily Water Intake.....	44
Hypertrophy of SON Somata and Nuclei following Partial Denervation.....	46
Morphometric Assessment of the Neural Lobe Vascular Plexus.....	53
Low Affinity (p75) Nerve Growth Factor Receptor Immunoreactivity in the NL.....	59
Morphometric Assessment of Glial Cell Numbers.....	66
DISCUSSION.....	73
Summary.....	90
REFERENCES CITED.....	92

## LIST OF TABLES

Table	Page
1. Size Distribution Bins of Vascular Morphometry.....	55
2. Results of Glial Cell Counts - Lesion Group Means.....	67
3. Results of Glial Population/Proliferation Estimates.....	71

## LIST OF FIGURES

Figure	Page
1. Oxytocinergic Perivascular Plexis Within the Hypothalamus.....	43
2. Effects of Unilateral Hypothalamic Lesion on Urine Osmolality.....	45
3. Effects of Unilateral Hypothalamic Lesion on Daily Drinking Volume.....	46
4. Effects of Unilateral Hypothalamic Lesion on Daily Urine Excretion Volume.....	47
5. Photomicrograph Demonstrating Silver-Enhanced Oxytocinergic SON Neurons.....	48
6. Hypertrophy of Vasopressinergic Neurons.....	49
7. Hypertrophy of Nuclei in Vasopressinergic Neurons.....	50
8. Hypertrophy of Oxytocinergic Neurons.....	51
9. Hypertrophy of Nuclei in Oxytocinergic Neurons.....	52
10. Effects of Lesion on Blood Vessel Density in the NL.....	54
11. Photomicrograph of NL Vasculature.....	56
12. Size Distribution of PS 2 Neural Lobe Vasculature.....	57
13. Size Distribution of PS 90 Neural Lobe Vasculature.....	58
14. Mean Proportional Area of NL Vasculature.....	59
15. Mean Proportional Area of NL Capillary Plexus.....	60
16. 192-IgG Immunoreactivity in the NL.....	61
17. Photomicrograph of NGFR immunoreactivity patterns in the NL at 5 days PS.....	62
18. Photomicrograph of NGFR Immunoreactivity Patterns in the NL at 90 days PS.....	64
19. Photomicrograph of Microglial Cells in the NL at 5 Days PS.....	65
20. Pituicyte Density in the NL.....	68
21. Pituicyte Nuclei Cross-Sectional Area.....	69
22. Microglia Density in the NL Following Surgery.....	70
23. Confocal Photomicrographs of GFAP/Brdu and GSA Lectin/Brdu Labeling in the NL at 5 Days PS.....	72

## ABSTRACT

Neuronal and non-neuronal correlates of compensatory sprouting in the neural lobe (NL) were investigated using a unilateral hypothalamic knife-cut of the hypothalamoneurohypophysial tract to partially denervate the rat NL. Metabolic, morphometric and immunocytochemical methods were employed to investigate the cellular activity which accompanies the magnocellular neurosecretory system's response to partial denervation. Analysis of the metabolic effects of partial denervation indicate a transient urine hypoosmolality within the first 24 hours post-surgery (PS) followed by a chronic urine hyperosmolality which persists throughout the 3 month investigative period. Daily water intake (drinking) and urine excretion volumes demonstrate drop below control levels immediately following surgery which persists throughout the investigative period. Morphometric measurement of the magnocellular oxytocinergic and vasopressinergic neurons in the contralateral supraoptic nucleus (SON) demonstrated an enlargement of both cell populations within 10 days PS which remained significantly above control levels for at least 30 days PS. These data also suggest the oxytocinergic cell population may enlarge more vigorously or at an earlier time than their vasopressinergic counterparts. Cell counts of glial cell nuclei within 1 micron coronal sections of the NL revealed an increase in the number of pituicyte nuclei by 2 days PS which remained above age-matched control values for at least 30 days PS. The number of microglial cell nuclei numbers increased by 2 days PS but returned to normal by 10 days PS. Morphometric analysis of the NL vascular plexis revealed a strong temporal correlation between the enlargement of the NL vascular plexis and the process of compensatory collateral sprouting of neurosecretory axons in the NL. Immunocytochemical analysis of bromodeoxyuridine (BrdU) substitution suggests that the microglial but not the pituicyte populations within the NL are undergoing hyperplasia between 1 and 6 days following partial denervation. Analysis of nerve growth factor receptor (NGFR) expression in the NL indicates a dramatic increase in the proportional area immunoreactive for NGFR between 5 and 10 days PS, which then returns to normal levels. Immunocytochemical comparison between NGFR, iC3b complement receptor and leukocyte common antigen (LCA) immunoreactivity suggest that a subpopulation of microglial cells may up-regulate their expression and/or increase the numbers of cells expressing the NGF receptor during a period when axonal degeneration and phagocytosis of neuronal debris is occurring. These data describe the varieties of neuronal and non-neuronal activities which underlie the compensatory axonal sprouting of intact magnocellular neurons within the partially denervated NL.

## INTRODUCTION

Statement of Purpose

These studies were designed to further elucidate the cellular correlates of the compensatory collateral sprouting which occurs within the magnocellular neurosecretory system (MNS) of the rat (Watt and Paden, 1991). The objectives of this research were to investigate the response of the MNS to partial denervation and to explore the non-neuronal activity associated with the initiation and maintenance of compensatory collateral sprouting of intact MNS axons following partial denervation of the neural lobe (NL). The goals were five fold. 1) Determine if the observed increase in relative area of partially denervated NL occupied by glia is due to cellular hypertrophy or hyperplasia of resident pituicytes and/or perivascular cells. 2) Investigate the possibility of a differential response in cellular activation/hypertrophy between oxytocin and vasopressin-immunoreactive cells in the contralateral supraoptic nucleus (SON). 3) Investigate the vascular response to partial denervation of the NL and its possible correlations with degeneration and sprouting of neurosecretory axons. 4) Evaluate the neurosecretory activity of vasopressinergic (VP) neurons by measuring alterations in drinking volume, urine excretion volume and urine osmolality. 5) Investigate the expression and possible up-regulation of nerve growth factor receptors (NGFR) on glial cells in the NL.

The first objective was accomplished in part by investigating the proliferative activity of pituicytes and/or perivascular cells. Glial involvement in central nervous system (CNS) disorders has been repeatedly demonstrated to occur in Alzheimer's disease (Mandybur and Chuirazzi, 1990), experimental allergic encephalomyelitis (Cammer et al., 1990) and muscular sclerosis (Lee et al., 1990). The data obtained in the present investigation may provide clues regarding the mechanisms

regulating the glial response to denervation and ultimately to improve our understanding of the glial role in CNS repair. The second goal was to investigate the role of neuronal activity in the sprouting response by comparing the response of oxytocin vs vasopressin MNS neurons to partial denervation of the NL. This was accomplished by comparing the extent and time course of cellular hypertrophy during the compensatory sprouting of vasopressin magnocellular neurons. The third goal was to investigate the response of the NL vascular plexus following partial denervation. As will be described below, the growth of the NL capillary plexus during axonal development and regenerative sprouting of severed neurosecretory axons appears to be required for successful axonal and terminal maturation. Therefore, a morphometric analysis of NL vasculature was undertaken to determine if growth of the NL capillary plexus correlates with axonal sprouting. The metabolic effects of partial denervation of the antidiuretic system, the MNS, were explored as a means of gaining an indirect estimate of circulating plasma VP levels and the relationship of plasma VP levels to the induction of the compensatory sprouting response of vasopressinergic axons. Finally, alterations in the expression of nerve growth factor receptors were measured immunocytochemically as a means of determining the contribution of perivascular microglial cells to the post-denervation response.

A brief historical review of the literature related to neural regeneration within the mammalian central nervous system will be presented next. This section will be followed by a detailed description of the structure and development of the neurosecretory system at both the light and ultrastructural level. This is intended to familiarize the reader with the close association of the components of the MNS and the interactions which underlie its development, function and inherent plasticity. This will be followed by a brief review of the different forms of injury-induced reorganization known to occur in the neurosecretory system and the contribution of nerve growth factor and

its receptors to CNS and neurosecretory function and response to injury. Finally, justification, rationale and specific aims will be presented.

#### Plasticity in the Mammalian CNS

Plasticity is a neurobiological concept which generally refers to the capacity of the central nervous system to modify existing synaptic contacts in response to injury, hormonal perturbations or environmental stimuli (Cotman et al., 1984). The principal evidence for plasticity comes from investigations of injury-induced responses (Cotman et al., 1984). Several forms of injury-induced axonal growth have been observed within the brain; these differ in several ways. First, regeneration generally describes the regrowth of a single fiber from the proximal end of the severed axon and is most frequently observed following injury to peripheral nerves. In the brain regenerative sprouting refers to the outgrowth of multiple collateral fibers from the proximal end of the severed axon. Second, the distance over which regrowth may occur is generally more extensive in regenerating axons than in sprouting axons (Cotman et al., 1984). Sprouts may arise from collaterals of intact fibers sharing the partially denervated terminal field (compensatory collateral sprouting), or from sustaining collaterals of injured axons proximal to the site of injury (regenerative sprouting; Kiernan, 1971). Injury-induced sprouting, often termed reactive synaptogenesis, may occur in several different forms, e.g., sprouts arising from nodes of Ranvier (nodal sprouting), from preexisting axon collaterals (collateral sprouting), or from the terminal bouton of intact axons innervating a partially denervated terminal field (terminal sprouting; Cotman et al., 1984). Although sprouting in any form can be extensive, it is generally more limited in the distance over which it may occur (Cotman et al., 1984), and tends to occur more rapidly (Murray, 1986) than regeneration.

Cellular events accompanying the sprouting process have also been observed. For example, cellular hypertrophy following injury has been

well documented. Following hypophysectomy both somata and nuclei of SON neurons hypertrophy paralleling the formation of a neural lobe-like structure in the proximal infundibulum (Moll and DeWeid, 1962; Raisman, 1973). Likewise, somata and cell nuclei of SON and paraventricular (PVN) neurons hypertrophy during compensatory sprouting of intact neurosecretory fibers in the NL (Watt and Paden, 1991). Such a response may be attributed to a heightened level of activity in the sprouting neurons (Moll and De Weid, 1962). Following unilateral ablation of the left striatum and overlying cortex Pearson et al., (1987a) described an increase in cell size in the contralateral pars compacta and ipsilateral pars reticulata of the substantia nigra, and the contralateral globus pallidus. These investigators also demonstrated hypertrophy of cholinergic cells of the rat basal forebrain following damage to the contralateral cortex. This enlargement was apparent by 7 days post-surgery and persisted for at least 300 days PS (Pearson et al., 1984). The degree of hypertrophy observed was related to the age of the animal (Pearson et al., 1985) and the degree of damage sustained (Pearson et al., 1987b). They went on to conclude that the hypertrophy represented a cellular response accompanying distal axonal sprouting (Pearson et al., 1987b). Cotman et al. (1977) have reported that increase in cell size is one of the earliest manifestations of the sprouting response. In several cases a correlation has been demonstrated between cellular hypertrophy and sprouting of intact efferents of the enlarged cells contralateral to the site of injury (Goldschmidt and Steward, 1980; Hendrickson, 1982; Headon, 1985; Pearson, 1987a), in a manner similar to that previously reported by the author (Watt and Paden, 1991). Thus, cellular hypertrophy in response to direct axonal injury or in response to partial denervation of a terminal field shared with other lesioned neurons is a well described cellular event.

### The Magnocellular Neurosecretory System

The magnocellular neurosecretory system (MNS) is composed of the large oxytocin and vasopressin-producing neurons of the paraventricular, supraoptic and accessory nuclei. The axons which originate from these neurons project through the ventromedial hypothalamus, median eminence and infundibular stalk to the neural lobe where they form synaptoid contacts with the outer basement membrane of the capillary plexus (Silverman, 1983; Ju et al., 1986).

The supraoptic nucleus is comprised of a compact mass of magnocellular neurons lying just anterolateral to the optic chiasm and optic tract (termed the principle division) (Ju et al., 1986), and a loose aggregation of magnocellular neurons positioned along the dorsolateral aspect of the optic tract and ventral surface of the brain at the level of the arcuate nucleus (termed the retrochiasmatic division) (Rhodes et al., 1981). There exists a partial segregation of vasopressinergic and oxytocinergic (OT) neurons within the principle division of the SON. The VP neurons are located predominately in the posteroventral region while the OT neurons are found predominately within the anterodorsal region (Vandesande and Dierickx, 1977; Rhodes et al., 1981; Swanson and Sawchenko, 1983).

The paraventricular nucleus, once thought to be a uniform aggregation of magnocellular neurons (Christ, 1969) is now known to be composed of 3 topographically distinct magnocellular and 5 parvocellular subdivisions (Armstrong et al., 1980; Swanson and Sawchenko, 1983; Silverman, 1983). The three magnocellular subgroups are described as the anterior, the medial and the posterior magnocellular subdivisions. The five parvocellular subdivisions are comprised of the anterior, medial, posterior, lateral and periventricular cell groups (Swanson and Sawchenko, 1983). A topographically distinct arrangement of VP and OT neurons also exists in the PVN. The anterior and medial magnocellular subdivisions are comprised almost exclusively of OT neurons. In the

posterior magnocellular subdivision the VP neurons are located predominately within the posterodorsolateral region and the OT producing neurons are found predominately in the anteroventromedial region (Swanson and Sawchenko, 1983).

In addition to vasopressin and oxytocin, at least 30 other neuropeptides have been immunocytochemically localized within the MNS including somatostatin, dynorphin, enkephalin, gastrin, and luteinizing hormone releasing hormone (Silverman, 1983; Swanson and Sawchenko, 1983; Ju, et al., 1986).

Retrograde transport studies utilizing horseradish peroxidase (HRP) injections into the neural lobe have further delineated the cell groups contributing terminals to the NL (Armstrong et al., 1980; Kelly and Swanson, 1980; Ju et al., 1986). Almost all of the cells of the SON are labeled following these injections. SON axons were seen rising in a fan-like array from the dorsal aspect of the principle division of the SON before coursing ventromedially toward the internal lamina of the median eminence (ME) and infundibular stalk. Axons arising from the more lateral regions of this division first course anterolaterally while the medially placed cells send axons anteromedially. Both groups then streamed caudally over the optic tract to join the fibers arising from the dorsal SON. Those axons originating from the retrochiasmatic division of the SON were seen to emerge from the dorsal aspect and stream medially, dorsolaterally and anterodorsally. However, only the anterodorsal axons were traceable for any distance and were seen to join their principle division counterparts along the dorsal surface of the optic tract (Ju et al., 1986).

The cell groups most heavily labeled within the PVN following retrograde transport of HRP from the NL are predominately concentrated within the medial and posterior magnocellular subnuclei (Silverman, 1983), corresponding to the PVM and PVL of Armstrong et al. (1980). However, scattered large and small neurons within several parvocellular

subnuclei are also labeled, with the periventricular division being the most substantial contributor (Swanson and Kuypers, 1980; Ju et al., 1986). The axons arising from the magnocellular divisions of the PVN project ventroposterolaterally from the PVN to course around the dorsal and ventral aspects of the fornix then sweep posteroventromedially to occupy the lateral horns of the zona interna of the median eminence on their way to the NL (Ju et al., 1986; Swanson and Sawchenko, 1983).

The magnocellular projections arising from the PVN and SON remain topographically segregated throughout their course through the hypothalamo-neurohypophysial tract. The SON efferents occupy the central two thirds of the zona interna, decussate within the median eminence, then continue through the infundibular stalk to form a widespread terminal distribution throughout the entire NL, with a higher concentration in the central core. The PVN fibers, on the other hand, maintain an ipsilateral distribution throughout their course through the lateral zona interna and infundibular stalk, and terminate primarily in the periphery of the NL (Silverman, 1983; Alonso and Assenmacher, 1981). The functional correlates, if any, of this anatomical separation remain unknown (Silverman, 1983). Silverman et al. (1980) have also reported reciprocal connections between oxytocinergic neurons of the PVN nuclei and between the ipsilateral PVN and SON nuclei. The regions receiving afferents from the contralateral PVN appear to be the PVL and PVM subnuclei (Silverman, 1983). Anatomical and electrophysiological evidence suggests the existence of bilateral polysynaptic (Takano et al., 1990) neural connections between the SON nuclei which may facilitate the synchronous firing of oxytocin and vasopressin neurons.

#### The Fine Structure of the Neural Lobe

The NL is traditionally described at the fine structural level as comprised solely of pituicytes, perivascular microglial cells, fenestrated vascular endothelia, the endothelial and parenchymal

basement membranes which delimit an extensive perivascular space, and the nerve fibers and terminals of neurosecretory axons. Within the confines of the perivascular space occasional fibroblasts and collagen fibrils may also be observed (unpublished observations). Axons arising from dopaminergic (Baumgarten et al., 1972; Saavedra et al., 1985) epinephrinergic and norepinephrinergic (Saavedra et al., 1985) and serotonergic neurons (Saland et al., 1987) have also been reported in the NL. However, the oxytocin and vasopressin neurosecretory axons comprise the vast majority of fibers pervading the NL. In the adult NL the neurosecretory axons are typically surrounded by the processes of pituicytes or completely engulfed within the pituicyte cell body. Rarely does one observe a "naked" axon within the NL. Likewise, the nerve terminal, when not in direct contact with the basement membrane, is ensheathed by pituicyte or parenchymal microglial processes.

There is no agreement yet on whether pituicytes occur in different forms or whether differing morphologies represent the same cell type in different functional states (Fugita and Hartman, 1961; Dellman and Owsely, 1969); Zambrano and De Robertis, 1968; Kruslovic and Bruckner, 1969). Dellman (1966) has described "dark" or fibrous pituicytes surrounding thin caliber axon cylinders in the proximal NL and a second "protoplasmic" pituicyte surrounding axonal swellings and terminals within the body of the NL. The "dark" pituicyte is characterized ultrastructurally by an electron dense cytoplasm, little perinuclear cytoplasm, thin processes, and an electron dense nucleus with abundant heterochromatin particularly clumped at the inner surface of the nuclear envelope. In contrast, the protoplasmic pituicyte has a distinctly thicker perinuclear cytoplasmic region, an electron lucent cytoplasm, thick processes, and a large round nucleus filled with euchromatin with only small amounts of clumped heterochromatin attached to the nuclear envelope. It is possible that these dark pituicytes represent a parenchymal microglial cell (see below) while the "protoplasmic

pituicytes" represent the only pituicyte population endogenous to the NL. This distinction may have important functional implications in the partially denervated NL.

A third cellular element endogenous to the NL, located within the perivascular space, is the perivascular microglial cell (Oliviere-Sangiaco, 1972). These cells are characterized by an elongate or oval nucleus displaying condensed heterochromatin clumped around the nuclear envelope, an electron dense cytoplasm, extensive granular endoplasmic reticulum, particularly in the perinuclear region but also extending into the long thin fibrous processes, lysosomes, numerous Golgi complexes and many free polyribosomes scattered throughout the cytoplasm (Oliviere-Sangiaco, 1972; Watt and Paden, 1991). The long processes extend throughout the perivascular space and are often observed to surround or partially envelop neurosecretory axons which have penetrated the outer basement membrane of the perivascular space (Oliviere-Sangiaco, 1972). Perivascular cells often contain dense inclusions and phagocytosed debris arising from the degeneration of neurosecretory axons in the normal animal (Oliviere-Sangiaco, 1972) and following unilateral destruction of the PVN (Zambrano and De Robertis, 1968) or SON (Watt and Paden, 1991).

#### Development of the Vascular Plexus of the Neurohypophysis

As a neurohemal organ, the neurohypophysis is characterized by an extensive penetrating vascular plexus. This plexus is composed in part by the border vessels located between the dorsal surface of the NL and the intermediate lobe (IL) and the superficial vessels which surround the remaining lateral and ventral external surface of the gland (D'Amore and Thompson, 1987; Eurenus, 1977).

The internal vascular plexus is thought to arise through an extensive invasive sprouting from the external vascular network during development of the NL. This development occurs in three principle

stages. The first stage lasts until fetal day 17, the second from fetal day 18 until the 10th day following birth, and the third from day 10 through day 30 (Galabov and Scheibler, 1978; Galabov and Scheibler, 1983). By 30 days of age the NL capillary plexus is thought to be fully mature (Galabov and Scheibler, 1983; D'amore and Thompson, 1987). Stage 1 is characterized by the development of the superficial and border plexuses surrounding the NL anlage, followed closely by the ingrowth of vascular sprouts at embryonic day 14 which arise from this peripheral network (Galabov and Scheibler, 1983). This vessel growth follows a distinct peripheral to central pattern of maturation. This pattern is opposite that of the maturation of neurosecretory axons which first penetrate the internal core of the NL then sprout toward the periphery (Galabov and Scheibler, 1978). During the early stages of vessel ingrowth, the perivascular space is typically very narrow and closely applied to the vessel wall. Ultrastructural analysis of the NL anlage at the later stages of the first developmental period show the NL to be packed with immature pituicytes. No morphological indications of functional activity, such as neurosecretory contacts or the presence of granules within the axons or pituicytes, are apparent by fetal day 17. Thus, in the first stage of NL development, the vascular development is clearly more advanced than that of the neurosecretory axons or pituicytes (Galabov and Scheibler, 1983). The second stage of NL vascular development is of particular interest as the first indications of functional activity become apparent (Galabov and Scheibler, 1978; Galabov and Scheibler, 1983). The inward penetration of vascular sprouts continues concurrent with the first appearance of endothelial fenestrae. Pituicytes show signs of continued maturation and functional activity and the perivascular cells have increased in size and numbers. The perivascular space, delimited by the parenchymal and endothelial basement membranes, widens, branches extensively, and extends deep into the NL parenchyma. The neurosecretory fibers in the central core of the

NL contain numerous granules and make contact with the outer basement membrane of the perivascular space (Galabov and Scheibler, 1983). During the ensuing days of fetal development, until the day of birth, the density of the vascular plexus increases considerably.

From the day of birth to the 10th day in the rat the vascular network continues to develop. Some immature capillaries are still observed within the central region of the NL but are few in number. There is an increased incidence of endothelial fenestrae and there are more fibrillar structures apparent within the perivascular space. At the beginning of this stage the pituicytes cover a large portion of the surface area of the perivascular basement membrane. However, as the second stage proceeds, these contact zones diminish as more neurosecretory axons establish terminal contact with the perivascular basement membrane (Galabov and Scheibler, 1983).

From 10-30 days of age the capillary network gradually attains the appearance of the mature animal. The perivascular cells appear to be highly active, as indicated by increased Golgi apparatus, and the general appearance of the perivascular space corresponds to that seen in the adult animal (Galabov and Scheibler, 1983).

The precise interrelationship between the development of the capillaries, pituicytes and neurosecretory axons remains unclear; however, it is of some importance to reiterate that the development of the capillary plexus precedes the ingrowth of the neurosecretory axons. Likewise, the appearance of endothelial fenestrae and widening of the perivascular space does not occur until contact is made between the neurosecretory axons and the basement membrane of the capillary network. These observations may indicate an inductive influence of the axons upon the final stage of maturation of the capillary plexus. Whether the initial growth of the capillary network has an inductive influence on the subsequent axonal growth also remains unresolved.

Neuronal Reorganization and Recovery of Function

If regeneration and sprouting represent forms of anatomical recovery from injury, the question arises whether or not such changes coincide with some degree of functional recovery. This is particularly relevant to the MNS since the regeneration of the proximal infundibulum, following hypophysectomy, leads to complete recovery of fluid balance. Although numerous studies have described some form of axonal reorganization following axotomy (eg., regeneration, sprouting of intact collaterals or sprouting of injured axons), relatively few studies have demonstrated a correlation between axonal growth and recovery of function (Finger and Almlı, 1985). In fact, the associations made between neural regrowth and functional recovery have been so sporadic that several opposing hypotheses have arisen regarding the underlying function of the reorganizational process. Some investigators maintain that the reorganizational process is strictly governed by the need of the system to achieve a level of function close to that maintained prior to the injury. Others suggest that the neural changes associated with injury are related to developmental processes and may result from an alteration in the balance between growth stimulating and growth suppressing factors (Finger and Almlı, 1985). Other investigators argue that any recovery of function associated with the reorganizational process is strictly coincidental. Support for the developmental hypothesis comes from studies of age-related factors and sprouting (Kawamoto and Kawashima, 1985a, 1985b, 1987). These studies have demonstrated that the initiation of the sprouting response is most rapid in the developing brain, decreases in the mature brain and is slower still in the aged brain (Cotman et al., 1984; Finger and Almlı, 1985).

If injury induced reorganization is related to a developmental process, it follows that this reorganization would be most likely to occur or to occur more rapidly during periods of rapid brain growth (Gall et al., 1981; Tsukahara et al., 1981; Cotman and Lynch, 1984;

Tsukahara, 1985). This does not, however, indicate that neural reorganization cannot take place in adult tissue. As mentioned above, there is ample evidence suggesting that mature systems do retain this ability but generally to a more limited extent (Steward et al., 1976; Cotman et al., 1977, 1984; Kawamoto et al., 1985; Needles et al., 1986). There are conditions under which sprouting in a previously denervated zone may contribute to recovery of function. Loecshe and Stewart (1975) demonstrated that unilateral damage to the entorhinal cortex resulted in initial impairment of performance of a trained task in rats; subsequently, task performance improved. Histologic examination demonstrated that sprouting had occurred within the contralateral entorhinal cortex and that the time course of sprouting was correlated with that of behavioral recovery.

Wuttke et al. (1977) reported functional recovery paralleling axonal regrowth in the anterior hypothalamus. Serotonergic input to the hypothalamus was interrupted using 5,7-dihydroxytryptamine (DHT) chemical axotomy. Initially there was a marked reduction in plasma luteinizing hormone (LH) levels; however, two months following surgery the LH levels returned to normal values. Axonal regeneration was evidenced by an increase in  $^3\text{H}$ -5HT uptake and release in the anterior hypothalamus which paralleled the recovery of LH levels.

Functional recovery following unilateral chemical axotomy of the descending serotonergic bulbospinal afferents was described by Nygen et al. (1974). Using the hindlimb extensor reflex as a measure of recovery, these investigators demonstrated that the initial 5-HT hypersensitivity observed following chemical axotomy disappeared within three months following surgery. This recovery was shown to closely parallel the time course of sprouting.

The prolific regrowth observed following damage to the axons of the magnocellular neurosecretory system has been repeatedly correlated with functional recovery (Raisman, 1977; Kawamoto, 1985; Kawamoto and

Kawashima, 1987). Hypophysectomy, the removal of the pituitary gland and distal infundibulum, is followed by the reestablishment of neurosecretory contacts with the capillaries of the mantle plexus in the zona externa of the median eminence (Raisman, 1977) and within the pseudo-neural lobe formed proximal to the stalk section (Kawamoto and Kawashima, 1987). Coincident with the development of these neurosecretory contacts, the polyuria and polydipsia associated with hypophysectomy disappear. The functional recovery achieved is such that the animal not only maintains homeostatic hydration levels but is able to resist moderate dehydration stress (Moll and DeWeid, 1962). Polenov (1974) found that salt loading hypophysectomized rats with a 1% NaCl drinking solution results in a substantial decrease in the amount of neurosecretory materials present within the proximal infundibulum. These animals demonstrate a direct correlation between alleviation of diabetes insipidus and release of secretory products from the reorganized neurosecretory endings. The functional competence achieved by the reorganized stalk was such that animals were able to withstand a twenty day salt loading regimen without deleterious effect.

#### Sprouting in the Magnocellular and Parvocellular Neurosecretory Systems

The magnocellular neurosecretory system has been the subject of extensive investigations of axonal sprouting in a variety of experimental preparations. Interruption of the hypothalamo-neurohypophysial tract either by hypophysectomy, neurolobectomy, infundibular stalk transection or hypothalamic lesion will result in morphological reorganization of the neurosecretory fibers proximal to the site of lesion in a variety of species. This effect was first described by Stutinsky in the rat (1951, 1952) and eel (1957). These initial reports were followed by further studies in the rat (Billenstein and Leveque, 1955; Moll, 1957; Moll and De Weid, 1962; Dellman and Owsley, 1969; Raisman, 1973; Polenov et al., 1974; Polenov et al., 1981;

Yulis and Rodriguez, 1982; Kawamoto and Kawashima, 1986, 1987), mouse (Kawamoto, 1985; Kawamoto and Kawashima, 1985), goat (Beck, et al., 1969), ferret (Adams, Daniel and Prichard, 1969), rabbit (Gaupp and Spatz, 1955), frog (Rodriguez and Dellman, 1970), Rhesus monkey (Antunes et al., 1978), and human (Beck and Daniel, 1959).

Following hypophysectomy the magnocellular neurosecretory axons which are normally confined to the internal zone of the median eminence grow ventrally into the external zone. Here they establish functionally competent contacts with fenestrated capillaries. These "synaptoid contacts" differ morphologically from axoaxonic, axodendritic or axosomatic synapses. The contact occurs between the terminal ending of the axon and the outer of two basement membranes enclosing the perivascular space. In an inactive state, these terminals are separated from the basement membrane by the active inclusion of a pituicyte foot process. Upon metabolic demand, the pituicyte withdraws and contact is reestablished. Hence these synaptoid contacts are dynamic and display an inherent functional plasticity in both the SON nuclei and neurohypophysis (Theodosis and Poulain, 1987). Ultrastructural examination found these neurosecretory contacts to be identical to those of the intact neural lobe (Raisman, 1977). Various investigators found that the neurosecretory axons reorganized into a miniature neural lobe-like structure at the proximal end of the transected infundibulum (Billenstein and Leveque, 1955; Moll and DeWeid, 1962; Kiernan, 1971; Raisman, 1973; Polenov et al., 1974; Kawamoto and Kawashima, 1987). Formation of new neurohemal contacts in both the ME and proximal infundibular stalk is accompanied by a general hypertrophy of the capillary mantel plexus (Raisman, 1973). A similar process has been described in ferrets (Adams et al., 1969) and mice (Kawamoto and Kawashima, 1985). The axonal growth observed in ferrets represents the most robust regenerative activity of neurosecretory axons yet observed.

Adams et al., (1969) severed the infundibular stalk in ferrets but

left the cut ends juxtaposed. A Gomori stain for neurosecretory material was then used to follow the course of regeneration from two weeks to twelve months. By two weeks the proximal portion of the lower infundibular stalk displayed clear indications of regenerating fibers having penetrated the scar tissue barrier. One to three months following surgery, the regenerating axons had grown as far as the caudal end of the infundibular stalk. By five months the regenerating fibers had invaded the neural lobe and in two animals sacrificed at one year post-surgery the entire neural lobe had been reinnervated. Several animals also developed a neural lobe-like structure just distal to the site of lesion. This growth is similar to the pseudo-neural lobe-like structure formed in the transected infundibular stalk following hypophysectomy.

Regeneration of severed MNS axons was also reported in rats following replacement of the neural lobe immediately after its removal, by suction, from the sella turcica. However, successful reinnervation of the neural lobe was only observed in two cases where the proximal infundibular stalk had not degenerated (Kiernan, 1971).

Silverman and Zimmerman (1982) have demonstrated a sprouting response within the parvocellular neurosecretory system following unilateral electrolytic lesion of the paraventricular nucleus in adrenalectomized rats. As described above, the parvocellular neurosecretory axons projecting from each PVN normally remain ipsilateral within their terminal field in the external zone of the median eminence (Alonso and Assenmacher, 1981; Silverman and Zimmerman, 1982; Vandesande et al., 1977; Antunes et al., 1977). Approximately 21 days following unilateral destruction of the PVN, however, both HRP injections into the intact contralateral PVN and immunocytochemical localization of vasopressin-neurophysin within the median eminence revealed a bilateral innervation of the external zone. The authors concluded that these previously undetected fibers arose through a

compensatory sprouting response of the undamaged terminals of the contralateral PVN efferents (Silverman and Zimmerman, 1982).

Regenerative sprouting of neurosecretory axons has also been demonstrated following interruption of the hypothalamo-neurohypophysial (HNT) tract within the hypothalamus (Danilova and Polenov, 1977; Antunes et al., 1979; Dellmann et al., 1985, 1986, 1987a, 1987b, 1988, 1989). However, growth occurs to a more limited extent than observed following interruption of the infundibular stalk (Danilova and Polenov, 1977; Antunes et al., 1970; Dellman et al., 1987a, 1988).

In the intact animal the neurosecretory fibers comprising the HNT tract normally do not form connections with the capillaries, venules or arterioles that traverse the hypothalamus (Antunes et al., 1979; Dellman et al., 1987a). However, following transection of the HNT neurosecretory axons, the proximal segments of these fibers will form new neurohemal contacts with newly formed vessels surrounding the lesion tract (Danilova and Polenov, 1977; Antunes et al., 1979; Dellman et al., 1987a) and with resident vessels of the hypothalamus not previously innervated by neurosecretory fibers (Antunes et al., 1979). Antunes et al. (1979) have reported such regeneration arising from both paraventricular and supraoptic neurosecretory axons, including oxytocin-neurophysin and vasopressin-neurophysin positive fibers. Exuberant growth of neurosecretory axons has also been observed in the ventral leptomeniges and surrounding pial vessels following disruption of the ventral hypothalamic surface (Danilova and Polenov, 1977; Antunes et al., 1979; Dellman et al., 1988). However, Antunes et al. (1979) reported observing hypothalamic sprouting no earlier than 8 weeks post-surgery (PS) while Dellman et al. (1987a) reported ultrastructural indications (e.g. the presense of morphologically defined neurosecretory granules with axon terminals) of perivascular sprouts surrounding hypothalamic lesion tracts and within the ventral leptomeninges as early as 5 days PS (Dellman et al., 1988). These fiber plexes were observed

within connective tissue spaces seemingly devoid of vessels, within arachnoid trabeculae and perivascular spaces, as well as surrounding the leptomeningial (pial) blood vessels (Dellman et al., 1988).

Unfortunately, Dellman's group did not discriminate between the two classes of neurophysins, precluding any direct comparison of sprouting efficacy of fibers containing vasopressin vs those containing oxytocin under these conditions.

Unsuccessful heterotypic tissue grafts placed within the hypothalamus are characterized by the absence of capillaries (Dellman et al., 1987b), underlying the essential nature of rapid revascularization for graft survival (Weigand and Gash, 1988). When NL allografts were positioned within the HNT, neurosecretory axons were observed invading the graft site within five days (Dellman et al., 1987b). Variations in the degree to which a graft was innervated were common and were correlated with the vascular density of the graft. In other words, graft sites containing the highest densities of vessels contained the highest numbers of neurosecretory fibers (Dellman et al., 1987b). During the initial stages of axonal invasion of the graft sites both terminal and preterminal neurosecretory fibers were observed. Preterminal fibers were typically found deeply invaginated into the perikaryon of pituicytes or completely enwrapped by pituicyte or "microglial-like" cell processes (Dellman et al., 1987b). Terminal fibers were less intimately associated with the pituicytes and were often observed abutting perivascular basement membrane (Wiegand and Gash, 1988) much as would be seen in the normal NL. However, as time passed, the axon-pituicyte relationship became more and more extensive (Dellman et al., 1987b).

Stereotaxic placement of intrahypothalamic allografts of sciatic nerve, optic nerve and hypodermal connective tissue within the HNT result in varying degrees of penetration by neurosecretory axons (Dellman et al., 1985a, 1985b, 1986a, 1987). The relative density of

invading neurosecretory axons appears to be dependent upon the degree of vascularization. Hence, NL allografts contain the highest number of axonal profiles while optic nerve allografts contain the least (Dellman et al., 1987b). However, within optic nerve allografts the highest density of neurosecretory fibers were always found in the immediate vicinity of blood vessels (Dellman et al., 1989). These observations indicate that the vasculature must play a prominent role in the attraction and maintenance of the neurosecretory axonal ingrowth. Although these data do not exclude the possible, and likely, contribution of pituicytes to the development and growth of neurosecretory axons in the normal animal, they do indicate the underlying importance of blood vessels and the various components of the perivascular network to a regenerative and/or compensatory sprouting response within the compromised neurosecretory system.

#### Nerve Growth Factor and its Receptors

Neuronal differentiation and survival in the developing and adult CNS is mediated by a variety of neurotrophic factors most notable of which is nerve growth factor (NGF). NGF is known to promote the survival and differentiation of neural crest-derived sensory neurons, sympathetic neurons and magnocellular cholinergic neurons of the rat basal forebrain (Williams et al., 1986; Taniuchi et al., 1986) and striatum (Martinez et al., 1985; Mobely et al., 1985). The highest levels of NGF protein and its message are found in those brain regions receiving the most dense cholinergic innervation: the cortex and hippocampus (Springer, 1988). Direct evidence indicating the contribution of NGF to survival and function of basal forebrain cholinergic neurons has emerged from studies of hippocampal plasticity. Unilateral lesion of the fimbria-fornix results in loss of innervation arising from the magnocellular cholinergic neurons of the basal forebrain. Concurrent with the degeneration of the cholinergic

terminals is a substantial rise in levels of nerve growth factor (NGF) protein, but not mRNA, within the denervated hippocampus within 10 days of axotomy (Larkfors et al, 1987; Korshing et al., 1986). Since only the protein and not the message increased, it has been suggested that this increase is due to the loss of cholinergic efferents which retrogradely transported the NGF protein away from the hippocampus. With the subsequent collateral sprouting of cholinergic fibers within the denervated field, the NGF protein levels return to normal (Milner and Loy, 1980). As a result of the axotomy the cholinergic neurons of the basal forebrain degenerate. However, chronic ventricular infusion of NGF (Hefti, 1986; Williams et al., 1986) or transplantation of NGF secreting tissues (Springer et al., 1988) will result in the survival of the axotomized neurons. These data indicate the reliance of specific central neurons in the adult brain on NGF for survival and plasticity.

Although the mechanism underlying NGF activity within a target tissue remains enigmatic, it is known that the ability of a target tissue to utilize NGF is reliant upon the presence of high affinity nerve growth factor receptor (NGFR) (Springer, 1988). At least two forms of the receptor exist: a high affinity form which is absolutely required for the internalization and utilization of NGF by the receiving cell, and a low affinity form which binds NGF but does not internalize the resulting NGF-NGFR complex, a step that is essential for NGF activity (Bernd and Greene, 1984; Hosang and Shooter, 1987; Johnson et al., 1988). Autoradiographic mapping of  $I^{125}$  NGF binding has demonstrated high affinity NGF receptors in the basal forebrain (Bernd et al., 1988), the caudate putamen, and most sympathetic and primary sensory neurons (Richardson et al., 1986). Immunocytochemical analysis and immunoprecipitation assays have demonstrated NGF receptors in the olfactory tubercle, medial septal nucleus (Taniuchi et al., 1986), the vertical and horizontal limbs of the diagonal band of Broca, the basal nucleus of the forebrain (Kiss et al., 1988), Purkinje cells of the

cerebellum (Taniuchi et al., 1986; Piore and Cuello, 1988), brainstem, cortex, hippocampus (Taniuchi et al., 1986), suprachiasmatic nucleus (Sofroniew et al., 1989), and posterior pituitary (Yan and Johnson, 1990) of the rat. Hence, there is a growing body of evidence implicating NGF activity and NGFR expression throughout the adult CNS.

A growing number of non-neuronal tissues and cell types, not believed to be NGF responsive, have been shown to express the low affinity form of NGF receptor and/or the NGF protein during development, following injury, or in cell culture. These include Schwann cells (Taniuchi et al., 1986; Johnson et al., 1988; Assouline and Pantazis, 1989; Matsuoka et al., 1991), cultured astrocytes (Furukawa et al., 1986; Yoshida and Gage, 1991), fibroblasts (Furukawa et al., 1985; Yoshida and Gage, 1991), and activated microglia (Yoshida and Gage, 1991). Fibroblasts will secrete NGF but have not been shown to express NGF receptor in rat or human (Assouline and Pantazis, 1989). CNS astrocytes also express NGF message (Lu et al., 1991) and protein, but not the NGF receptor, (Assouline and Panatazsis, 1989) in culture (Yoshida and Gage, 1991), during development and following axotomy of the optic nerve of the adult rat (Lu et al., 1991). In vitro studies have demonstrated the expression of NGF to be highest during stages of rapid glial growth (Yoshida and Gage, 1991).

Non-neuronal cells express only the low affinity form of the NGF receptor (Johnson et al., 1988) and are not capable of internalizing or utilizing the NGF protein. The expression of NGF receptors and secretion of NGF protein by Schwann cells is developmentally regulated (Johnson et al., 1988). Binding of NGF occurred from days E6-E16 of development. After this stage the receptor expression diminished to undetectable levels (Johnson et al., 1988). However, following peripheral axotomy a reexpression of low affinity NGF receptor by the ensheathing Schwann cells (10-50 fold) appeared within 3 days and peaked at 5-7 days (Taniuchi et al., 1986; Johnson et al., 1988). The

reexpression was confined to the region distal to the lesion. No reexpression was detected proximal to the lesion where axon-Schwann cell contact remained, indicating a contact mediated suppression of NGF receptor expression by Schwann cells (Johnson et al., 1988). The presentation of bound NGF on the surface of the Schwann cell (presumably secreted by the same Schwann cell) may play a role in the cell's contribution to axonal regeneration following axotomy by providing an NGF-lined path for the regenerating axon to follow (Johnson et al., 1988). Once the regenerating axon reached its NGF secreting target tissue, NGF secretion and expression of NGF receptors were shut off.

Within the posterior pituitary of the neonatal rat, NGF receptor expression (detected immunocytochemically) continues to intensify in expression throughout the first year of life (Yan et al., 1990). Following transection of the pituitary stalk, the NGF receptor immunoreactivity rose dramatically within 3 days and peaked at approximately 15 days following stalk transection (Yan et al., 1990). This correlates closely to the time when axon degeneration was occurring and phagocytosis of the axonal debris was at a maximum. Dehydration, lactation, castration in male rats, pregnancy and colchicine injection all produced alterations in glial and/or neurosecretory activity in the neural lobe. However, none of these manipulations resulted in an increase in NGF receptor immunoreactivity. These data would suggest that the increased glial activity associated with phagocytosis of the axonal debris was responsible for the increase in NGFR immunoreactivity. The cell type within the neural lobe thought to be responsible for phagocytosis is the perivascular microglial cell (Zambrano and Robertis, 1979; Watt and Paden, 1991).

In summary, the occurrence of NGF and NGF receptors has been repeatedly demonstrated in both neuronal and non-neuronal cells of the peripheral and central nervous systems. Within the adult CNS the role of NGF and NGF receptors remains unresolved. Indications of up

regulation of NGF protein and receptor following axotomy reflect a potential for CNS repair similar, but more limited in extent, to that observed in the peripheral nervous system.

#### Justification, Rational and Specific Objectives

##### Role of Glia in Axonal Sprouting.

The proliferative astroglial response to penetrating injury often leads to inflammation and the development of scar tissue which may act as a barrier to axonal regeneration. However, there is accumulating evidence to suggest that astroglia and microglia may also play a supportive role in axonal sprouting, typically under conditions in which inflammation, tissue insult and disruption of the blood-brain barrier do not occur (Gall et al., 1979; Gage et al., 1988). The principle advantage of our model of collateral sprouting (Watt and Paden, 1991) is that the use of a unilateral hypothalamic knife cut, instead of an infundibular stalk section, hypophysectomy or neural lobectomy, permits the sprouting response of uninjured neurons to be studied in the intact NL without the complications arising from hemorrhage or scar formation. The NL in turn offers a highly simplified tissue, of CNS origin but lying outside the blood-brain barrier, in which to investigate problems such as the role of glial and neuronal activation in the sprouting response of central neurons.

At least two distinct populations of glial cells reside within the NL, pituicytes and perivascular cells. Immunocytochemical application of an antibody directed against glial fibrillary acidic protein (GFAP), a known astrocyte-specific marker, indicates pituicytes are GFAP-positive and thus an astroglial-like cell (Velasko et al., 1979; Suess and Pliska, 1981; Salm et al., 1982). Pituicytes are characterized by highly asymmetric and extensive processes in close juxtaposition to neurosecretory axons and have a more velate appearance compared to astrocytes (Salm et al., 1982). Although the functional role of

pituicytes remains unresolved, they are known to ensheath axonal endings within the NL when these axons are not in contact with the external basement membrane of the perivascular space. However, upon stimulation of the anti-diuretic system the pituicytes will rapidly withdraw from the axon terminals allowing terminal/basement membrane contact for neurosecretion. Additionally, pituicytes will cover the basement membrane left exposed upon axon terminal retraction (Wittkowski and Brinkman, 1974). We believe the intimate relationship between pituicytes and axons may be crucial in the sprouting response. A similar contiguous relationship between pituicytes and axons has been reported in the developing NL (Galabov and Scheibler, 1978; Dellman and Sikora, 1981) and during regenerative sprouting in the proximal infundibulum (Kiernan, 1971).

NL perivascular cells are thought to be related to CNS microglia (Fugita and Hartman, 1961; Zambrano and de Robertis, 1968). Microglia, in turn are thought to be of mesenchymal origin and thus are not related to neuronal or neuroglial elements which arise from the germinal matrix (Dickson and Mattiace, 1989). Antibodies which recognize mesodermally-derived elements such as macrophages will also recognize microglia (Perry et al., 1985; Giulian et al., 1976; Esiri and McGee, 1986; Hickey and Kimura, 1986). Likewise antibodies directed against major histocompatibility complex (MHC) class II, commonly detected on immune cells, will also recognize microglia (Dickson and Mattiace, 1989). However, microglia can be distinguished from tissue macrophages and blood monocytes on the basis of histochemical, morphologic and mitogenic analyses (Giulian et al., 1986). Our data indicate a functional relationship between perivascular cells of the NL and activated macrophages. We have observed that perivascular cells are solely responsible for phagocytosis of degenerating neurosecretory axons following knife cut (Watt and Paden, 1991). This activity is apparent at 5 days following knife cut and is characterized by an apparent

increase in the number of perivascular cells within the NL, an increase in the number of electron dense cytoplasmic lysosomal granules, highly dilated rough endoplasmic reticulum (RER) filled with a dense amorphous material and the presence in some perivascular cells of phagocytic debris (Watt and Paden, 1991). Likewise, Zambrano and De Robertis (1968) have shown perivascular cells to be exclusively involved in the phagocytosis of degenerating neurosecretory axons within the NL following bilateral electrolytic destruction of the PVN.

Neuroglia and microglia may play an important role in neural repair following injury. Hypertrophy of astrocytes occurs surrounding sites of brain injury and neuronal death (Jacobson, 1978) as does proliferation of astrocytes in proximity to the site of an injury (Cavanagh, 1970; Latov et al., 1979). Microglia proliferate at a very high rate within 2-5 days following axotomy of the facial nerve (Kreutzberg and Barron, 1978) and within the outer molecular layer of the hippocampus following partial deafferentation (Gall et al, 1979). In this instance the proliferation of microglial cells preceded the increase in numbers of astrocytes. This sequential pattern is supported by evidence suggesting microglial cells secrete factors involved in the proliferation of astrocytes (Giulian and Baker, 1985). Furthermore, production of "glia-promoting factors" can be elicited by brain injury (Giulian et al, 1976). The possibility remains that the perivascular cells of the neurosecretory system are in fact a form of microglial cell. If so, it would seem likely that these cells would express immunologic cell surface markers as do microglia and macrophages (Perry et al, 1985; Esiri and McGee, 1986; Hikey and Kimura, 1988; Dickson and Mattiace, 1989). Likewise, immunopositive staining of pituicytes with GFAP indicates that these cells are at least related to, and possibly share a common ontogeny with, brain astrocytes. If so, the relationship between these cell types in the neural lobe may closely parallel that observed between the microglia and astrocytes of the brain, particularly

in response to brain injury or neuronal death.

My working hypothesis is that the degenerative debris resulting from axonal degradation stimulates the activation, proliferation and phagocytic response of perivascular cells. This phase is followed by the activation, hypertrophy and possible proliferation of resident pituicytes, possibly as a result of one or more factors released by the activated perivascular cell population. The focus of this investigation was on the hypertrophy and hyperplasia of the glial population.

#### Neuronal Activation in Collateral Sprouting.

Cellular hypertrophy has been repeatedly demonstrated to correlate with the onset of compensatory sprouting of intact afferents to a partially denervated site in a variety of CNS systems (Goldschmitt and Steward, 1980; Headon et al., 1985; Hendrickson and Dineen, 1982; Pearson, et al., 1987a; Pearson, et al., 1987b). Likewise, hypertrophy of SON neurons has been demonstrated to occur concomitant with the reformation of neurosecretory nerve terminals in the proximal infundibulum following hypophysectomy (Raisman, 1987). We have demonstrated that hypertrophy of magnocellular neurons in the contralateral SON coincided with the increase in axon number observed at 30 and 90 days following partial denervation of the NL (Watt and Paden, 1991). These observations are consistent with the conclusion that compensatory sprouting of intact neurosecretory efferents was occurring at this time. Cellular hypertrophy in the magnocellular neurosecretory system has also been associated with heightened secretory activity induced by dehydration or salt loading (Enestrom, 1967; Morris and Dyball, 1974; Peterson, 1966). However, these acute effects occur rapidly, and the somata return to normal size soon after cessation of the osmotic stimulation (Enestrom, 1967; Morris and Dyball, 1974). In contrast, the prolonged delay observed in our study between partial denervation of the NL and the increase in cell size suggests the

cellular enlargement is not the result of increased vasopressin synthesis or secretion.

We believe the increase in SON and PVN cell size observed may reflect the increased cellular metabolic activity required to maintain an enlarged terminal arbor. Furthermore, this enhanced activational state may be a critical factor in determining the extent of the regenerative response. Herman and Gash (1987) demonstrated that vasopressinergic, vs oxytocinergic, cellular activity following NL ablation could be selectively inhibited via chronic vasopressin infusion. Results of their study suggest inhibition of vasopressinergic cell activity inhibits axonal regeneration and ultimately results in cell death, with no effect on the activational state, cell survival, or regenerative capacity of the axotomized oxytocinergic neurons. These results indicate the critical importance of heightened cellular activity to regenerative capacity (although, the specific form of activity, e.g., gene expression, synthetic, or electrophysiological, remains unclear). An advantage of the MNS as a model system for the study of sprouting is the possibility of selectively activating and suppressing vasopressinergic or oxytocinergic cell activity using different hormones, (e.g., vasopressin and oxytocin), and different physiological states (e.g., pregnancy, lactation, dehydration). Other investigators have demonstrated a difference in the temporal pattern of vasopressin and oxytocin immunoreactivity in the median eminence following hypophysectomy relative to the onset of sprouting of vasopressin axons as a function of age in both rats (Ibata et al., 1983; Kawamoto and Kawashima, 1987) and mice (Kawamoto, 1985). These findings suggest that there may well be differences in the ability of oxytocin vs vasopressin cells to undergo compensatory sprouting. The basis of such differences and their relation to cell activity remain unknown. I proposed to explore this problem by determining the temporal pattern of oxytocin vs vasopressin neuronal hypertrophy in the contralateral SON and its

possible correlation with the onset of compensatory sprouting by oxytocin and vasopressin axons in the partially denervated NL. Further exploration of any differences in vasopressin vs oxytocin neuronal activation and sprouting may provide new information regarding factors that affect the neuronal propensity for compensatory sprouting.

Specific Objectives. A novel model of compensatory collateral sprouting of intact magnocellular vasopressinergic efferents following partial denervation of the rat NL has been reported (Watt and Paden, 1991). In addition to the sprouting response, further analysis revealed an increase in the relative area of the NL occupied by glial cells. This increase corresponded to the period of degeneration, activation of the vasopressinergic neurons and onset of sprouting. My objectives are divided into two principle areas of investigation: 1) to further investigate the role of non-neuronal elements in the facilitation, initiation, and/or maintenance of the compensatory sprouting response and, 2) to measure the neuronal response to partial denervation and possible correlations with the sprouting response.

These data may provide clues regarding the mechanisms regulating the glial and neuronal response to denervation and ultimately to improve our understanding of the glial role in central nervous system (CNS) repair. The specific aims of the proposed research and hypotheses to be tested are as follows:

Non-Neuronal Contribution to MNS Response to Injury 1) To determine if the observed increase in relative area of partially denervated NL occupied by glia is due to cellular hypertrophy of resident pituicytes and/or perivascular cells or to a proliferative response resulting in an increase in the absolute number of cells in either glial population. 2) To determine the vascular response to partial denervation of the NL and its possible correlations with degeneration and sprouting of neurosecretory axons.

3) To investigate the expression and possible upregulation of NGF receptors on glial cells in the NL.

Neuronal Activity 1) To investigate the possible occurrence of regenerative sprouting of neurosecretory axons within the hypothalamus.

2) To investigate the possible alterations in drinking volume, urine excretion volume and urine osmolality as an indirect means of determining whether the sprouting response may result from a lesion-induced deficit in plasma vasopressin levels.

3) To determine if a differential response in cellular activation/hypertrophy exists between oxytocin- and vasopressin-immunoreactive cells in the SON.

## METHODS

Animals

Male Holtzman rats (bred from stocks originally obtained from Charles River) were 35 to 40 days of age at the time stereotaxic surgery was performed. The sprouting efficacy of transected neurosecretory axons has been shown to decrease with age (Kawamoto and Kawashima, 1985, 1987) and this reduced propensity has been observed as early as 23 days post-parturition (Kawamoto and Kawashima, 1987). Therefore, young rats between the ages of 35-40 days post-parturition were utilized in an effort to minimize any age-related impairment of the neurosecretory system response to partial denervation. Animals were either individually or group housed under a 12L:12D light cycle and had ad lib access to lab chow and tap water throughout the investigations.

Surgery

Prior to surgery each animal received Sodium-Pentobarbital, (50mg/kg intraperitoneal (IP)) to induce a surgical plane of anesthesia. Animals received methoxyflurane to prolong or deepen the plane of anesthesia, as necessary. Each animal received a preanesthetic injection of atropine sulfate, 0.5mg subcutaneous (SC), to reduce mucous secretions. Following anesthesia, the heads were shaved, washed with 100% ethanol (ETOH) and positioned in the stereotaxic apparatus with the incisor bar set at 3 mm below the horizontal position. Incisions were then made in a caudal to rostral direction and the dorsal surface of the cranium exposed, cleared of fascia and dried. The tip of the stereotaxic knife blade (see appendix for materials and design), was positioned at bregma and the coordinates recorded. The lesion coordinates, AP -3mm to +5mm, ML -0.5mm, (Paxinos and Watson, 1986) were then marked on the surface of the cranium with bregma serving as stereotaxic zero. A burr hole was then made through the skull using a

Dremel moto-flex drill and a #3 carbide burr, with care taken to ensure that the hole had clean, smooth edges to reduce the possibility of scalp irritation after surgery. The dura mater was incised using a sterile, 27 gauge hypodermic needle. Any excessive bleeding was interrupted by applying direct pressure with a Kimwipe pad directly to the wound site. Once the incision was completed and cleared of debris, the stereotaxic knife blade was then repositioned at -2mm AP, and lowered through the brain to the ventral surface of the cranial cavity. When the knife blade contacted the skull surface, the blade flexed slightly. The blade was then retracted 1mm and the knife slowly brought forward to the rostral extent of the lesion. The blade was then retracted and any blood and/or debris was cleared from the site. The wound was closed by first filling the burr hole with Gelfoam. The surface of the cranium was then gently wiped clean and nitrofurazone topical antibiotic applied liberally, and the scalp sutured. The animal was then removed from the stereotaxic apparatus and replaced in his home cage for recovery. All sham controls were prepared in a like manner except that the knife blade was lowered only 4 mm from the dorsal surface of the skull. This lesion depth transected the cortex but did not impact the hypothalamus, thus sparing the PVN and SON nuclei from damage.

#### Tissue Preparation

Tissue was collected from groups of experimental animals sacrificed between 12 hours and 150 days PS as well as from age-matched sham-operated and intact controls. Animals to be used for morphometric analysis of immunocytochemically-labeled vasopressin and oxytocin neurons of the SON were perfused intracardially with 4% paraformaldehyde in .1M phosphate buffer under deep ether anesthesia, then decapitated and the brain and NL removed. The brain and attached NL were then submerged and postfixed in the perfusion medium overnight, then dehydrated, cleared in xylene and embedded in paraffin. Animals to be

used for Bromodeoxyuridine (BrdU) substitution analysis were first placed under light ether anesthesia and then given a 1 ml IP injection of 20.0 mg/ml BrdU in .007M NaOH vehicle. Animals were allowed to survive for three hours following injection and then were perfused intracardially with saline solution for three minutes under deep ether anesthesia. The brain and attached NL were removed and immersion fixed with Carnoy's acidified alcohol fixative overnight. The tissue was then dehydrated for 3 hours in absolute ethanol, cleared for three hours in xylene and embedded in paraffin.

Animals involved in the capillary morphometry and glial population estimates were anesthetized with ether and then perfused intracardially with 4% paraformaldehyde plus 2% glutaraldehyde in .1M phosphate buffer. The NL was then removed and postfixed overnight in the perfusion medium, then dehydrated, cleared in xylene and embedded in paraffin. The NL was postfixed 4 hours in 2% osmium tetroxide, dehydrated in ethanol and propylene oxide and then embedded with Spurr's epoxy resins in flat-mount Beem capsule molds with the rostral end of the NL positioned at the tip of the Beem capsule for orientation.

Tissues to be utilized for immunohistochemical analysis of the p75 low affinity nerve growth factor receptor (NGFR) were first perfused intracardially under deep ether anesthesia with cold saline for two minutes and then perfused for 20 minutes with Nakane's periodate-lysine-paraformaldehyde (PLP) fixative. The PLP fixative containing 2% paraformaldehyde, .075M lysine and .01M sodium periodate in .1M  $\text{PO}_4$  was prepared immediately before use. Following perfusion, the brain and NL were removed intact and postfixed overnight in PLP, cryoprotected in 30% sucrose/PBS for 24-48 hours at 4°C and then snap frozen in molds filled with OCT freezing compound using isopentane chilled to -160 degrees centigrade in liquid nitrogen. The tissues were then stored at -70 degrees centigrade until sectioned. Once sectioned and mounted on gelatin-coated slides, the sections were stored at room temperature.

### Tissue Microtomy

Paraffin microtomy was performed on a Leitz Wetzlab microtome. For the investigation of SON neuronal hypertrophy ten micron serial sections were collected from each specimen block, float-mounted singly on gelatin coated slides and dried overnight on a slide warmer prior to use. Those sections utilized for Brdu analysis were sectioned at six microns and mounted in a similar manner. All fresh frozen tissues for NGFR analysis were sectioned at ten microns using a Reichert-Jung Frigocut 2800 cryostat and thaw mounted on gelatin-coated slides.

For capillary morphometry and glial nuclear counts one micron semithin sections of Spurr's embedded NL were sectioned using a Reichert Nr 318 435/E ultramicrotome using glass knives and collected from each of four subject animals per lesion group and three animals per age-matched control group. Sections were mounted on gelatin-coated microscope slides by placing each section on a drop of distilled water and then drying briefly on a slide warming tray. All sections on a given slide were then coated with a liberal volume of 1% basic toluidine blue and warmed for approximately 5-7 minutes before being rinsed in distilled water. The staining intensity was then adjusted by brief immersion of the slide in 95% and 100% ethanol and coverslipping with Permount.

### Immunohistochemistry

In a previous investigation we were able to demonstrate hypertrophy of SON and PVN neurons and their respective nuclei which coincided with the collateral sprouting response of vasopressinergic neurosecretory axons (Watt and Paden, 1991). However, the Nissl stain utilized to visualize these neurons did not allow for a direct comparison between the vasopressin- and oxytocin-immunoreactive neurons within either nuclei. Therefore, the possibility of a differential response between vasopressin and oxytocin immunoreactive neurons within

the SON was investigated by selectively immunolabeling each of the two neuronal populations for subsequent morphometric analysis. Both peroxidase and silver-intensified immunogold preparations were utilized in an effort to produce the most sensitive and accurate estimation of neuronal size, as described in detail below.

Immunohistochemical application of anti-vasopressin-neurophysin (gift of Dr. Alan Robinson) and anti-synthetic oxytocin (Accurate) was performed on paraffin-embedded coronal sections from each of three experimental groups (6-8 animals/group) and four intact control groups (4 animals/group). The intact groups were included to control for any age-related increase in neuronal and/or nuclear size. The number of sections prepared for each animal was solely dependent on the number required to measure a minimum of 25 cell bodies and their respective nuclei in each animal. Most animals, however, had 35 to 50 cell bodies and nuclei measured. Sections were cleared of all traces of paraffin and then rehydrated through decreasing concentrations of ethanol leading to phosphate buffered saline (PBS). All sections were then incubated in either rabbit anti-vasopressin-neurophysin (1:1000) or rabbit anti-synthetic oxytocin (1:2000) in blocking serum composed of bovine serum albumin and normal goat serum, pH 7.4, overnight at room temperature in a plastic hydration chamber. Sections were then rinsed in PBS for two successive ten minute increments and exposed to the secondary antibody, biotinylated goat anti-rabbit IgG (1:200) (Cappel) for one hour at room temperature in a hydration chamber. Sections were again rinsed twice in PBS then incubated in avidin-biotin complex (ABC) (Vector) for one hour as before. Finally, all sections were rinsed in PBS and then developed in 3,3' diaminobenzidine (DAB) (Sigma) solution containing 300  $\mu$ l of 1 mg/ml glucose oxidase and 600  $\mu$ l of 1% cobalt chloride per 100 ml of DAB solution.

Silver-enhanced immunohistochemistry was performed as follows. Sections were cleared of paraffin in xylene and then rehydrated through

successive decreasing concentrations of ethanol to tris-phosphate buffered saline (TPBS) pH 7.4. All sections were then incubated for one hour in TPBS blocking serum (GSTPBS) containing 3.0% normal goat serum. The GSTPBS was then wicked away using Kimwipes and the primary antisera, rabbit anti vasopressin-neurophysin (1:40,000) (gift of Dr. Alan Robinson), was applied and left overnight at room temperature in a plastic hydration chamber. All sections were then washed for 60 minutes in GSTPBS and the secondary antibody, goat anti-rabbit IgG conjugated to a 1 nm gold particle (BioCell), was applied and incubated at room temperature for 60 minutes. All sections were then washed in GSTPBS for 60 minutes and then washed for 10 additional minutes in sterile water (pyrogen-free for injection) (Kendall McGraw). Sections were washed in .2M citrate buffer, pH 3.85, for 10 minutes to slow the rate of silver deposition. Sections were then placed in a silver development solution which was prepared by combining 15 mls of 5.6% hydroquinone in sterile water, 15 ml of 0.7% silver lactate in sterile water, 10 ml of 2.0M sodium citrate buffer (pH 8.5) and 60 ml sterile water. Sections were then developed under a sodium vapor lamp for 8-16 minutes or until the reaction was judged to be complete. The development reaction was then halted by replacing the silver solution with a 5% acetic acid stop bath for one minute, and then fixing the sections in Kodak fixer for 10 minutes. All sections were then washed in a continuous flow of tap water for 30 minutes, counterstained in a 1% working solution of cresyl violet (Aldrich) and coverslipped in Permount.

Low affinity (p75) nerve growth factor receptor (NGFR) expression in the NL was measured by applying the mouse monoclonal antibody 192-IgG (gift of Dr. E.M. Johnson, Jr.) to tissue sections selected from lesion and sham operated animals sacrificed at post-surgery days 0, 2, 5, 7, 10, 35 and 90. A minimum of 8 sections of NL were selected from each of 4-6 animals within each group. Tissue sections were selected from approximately the same depths through the NL across all animals in all

groups to ensure that a reasonably equivalent comparison was made between animals and between experimental groups. The large number of sections stained and the nature of the analysis (see below) required that sections be prepared in batches of 18. In order to ensure that variations in staining intensity not bias the analysis, each batch contained sections selected from animals representing both lesion and sham preparations from several time points. Sections were washed for 30 minutes in Tris-buffered saline and then incubated overnight with primary antibody 192-IgG (1:100) in TBS blocking serum (TBS/NHS), pH 7.6, containing 1% normal horse serum. All incubations were conducted at room temperature in a plastic hydration chamber. Following the primary antibody, the sections were washed for a minimum of two 10 minute intervals in TBS and then incubated with the secondary antibody, biotinylated horse anti-mouse (1:500)(Vector) in TBS/NHS, pH 7.6. Sections were then washed in TBS for two 10 minute intervals and incubated in ABC for 60 minutes. Again, sections were washed in TBS for two successive 10 minute intervals and then developed in DAB in darkness for 60 minutes. All sections were then washed for a minimum of ten minutes in TBS, dehydrated through increasing concentrations of ethanol, cleared in xylene and coverslipped in Permount.

Immunocytochemical analysis of Brdu substitution was performed to determine if the apparent increase in the number of pituicyte nuclei was due to cell mitosis. Cell counts indicated that this increase occurred as early as 24 hours following the knife cut. Therefore, animals injected with Brdu were sacrificed at .5, 1, 2, 3, 4, 6, 7, 10 and 30 days PS. Sham controls were sacrificed at 1, 2 and 10 days PS. As before, tissue sections were selected from approximately the same depths through the NL across all animals in all groups to ensure that a reasonably equivalent comparison was made between animals and between experimental groups. Selected sections were cleared of all traces of paraffin in xylene and then rehydrated through decreasing concentrations

of ethanol leading to PBS. Because the anti-Brdu antibody will recognize only single stranded Brdu substituted DNA, denaturation was performed by a 60 minute incubation in 2N HCL. The primary antisera, mouse anti Brdu (1:100)(Becton-Dickenson), diluted in blocking serum (PBS containing 1% bovine serum albumin (BSA) and 1% normal goat serum) was then applied and left overnight. All incubations were performed at room temperature in a plastic hydration chamber. Sections were then washed in two successive 10 minute PBS rinses and then exposed in succession to the secondary antibody, biotinylated goat anti-mouse (1:200) in blocking serum for 60 mins., two 10 minute PBS rinses, ABC for 60 minutes, two 10 minute PBS rinses, then .025% DAB containing .03% glucose oxidase solution (Sigma) with .03% cobalt enhancement for 15-20 minutes in darkness. Each section was then counterstained in Gill's Hematoxylin, dehydrated through a series of increasing concentrations of ethanol, cleared in xylene and coverslipped in Permount.

Once having determined that Brdu substitution had occurred, it was necessary to identify the proliferative cell type(s). This was accomplished by utilizing both dual-label immunofluorescence and dual-label peroxidase immunocytochemistry. Immunofluorescent preparations were subsequently analyzed utilizing confocal microscopy.

For dual fluorescence immunocytochemistry, selected sections were cleared of all traces of paraffin in xylene and then rehydrated through decreasing concentrations of ethanol leading to PBS. Sections were then incubated in 2N HCL for 60 minutes, followed by three 10 minute PBS washes. The primary antisera, both mouse anti-Brdu (1:100)(Becton-Dickenson), and rabbit anti-glial fibrillary acidic protein (GFAP)(1:250)(Dako) were diluted in blocking buffer (containing 1% (BSA) and 1% normal mouse serum), was then applied and left overnight. All incubations were performed at room temperature in a plastic hydration chamber. Sections were then washed in two successive 10 minute PBS rinses and exposed in succession to: biotinylated goat anti-mouse

antibodies (b-GAM) for 60 minutes, two 10 minute PBS washes, an avidin-phycoerythrin (1:200) (Avidin-PE) (Accurate-Phycoprobe) and fluorescein isothiocyanate-goat anti-rabbit (1:500) (FITC-GAR) (Hyclone) solution for 60 minutes, and two 10 minute PBS washes. Slides were then coverslipped in PBS:glycerol with 1mg/ml O-phenylenediamine.

For dual label peroxidase immunocytochemistry the sections were cleared, rehydrated and denatured as described above and then exposed to the following sequence: anti-Brdu (1:100) overnight at room temp., 2x10 min PBS washes, b-GAM (1:200) for 60 minutes at room temp., 2x10 min PBS washes, ABC for 60 minutes, room temp., 2x10 min PBS washes, development in DAB with cobalt enhancement for 15-20 minutes, PBS wash for a minimum of 30 minutes, the second primary antibody (e.g. anti GFAP overnight at room temp.), 2x10 min PBS washes, secondary antibody b-GAR (1:200) for 60 minutes at room temp., 2x10 min PBS washes, ABC for 60 minutes at room temp., 2x10 min PBS washes, DAB without cobalt enhancement for a 15-30 min development period, followed by a PBS wash, dehydration, clearing and coverslipping in Permount. This paradigm resulted in a highly compartmentalized and very black Brdu nuclear staining against a ruddy brown cytoplasmic GFAP staining, allowing the two antibody staining patterns to be easily discerned and compared.

#### Image Analysis and Morphometric Measurements

##### 192-IgG Proportional Area Analysis

Quantification of 192-IgG immunopositive proportional area was performed on an MCID image analysis system (Imaging Research Inc.). Microscope illumination was stabilized with a SOLA CVS transformer to prevent fluctuations in illumination intensities from biasing measurements of the 192-IgG immunopositive area. Caution was taken when reaccessing the MCID program that illumination intensities and microscope aperture settings were precisely the same as for all previous sessions. Calibrations were checked prior to each sampling

session against a known sample. Images were projected from an Olympus BH-2 light microscope using a 10x objective through a Sierra Scientific CCD high resolution camera for relay to the MCID program and displayed on an Electrohome monitor for image editing and analysis.

The 10X objective was the lowest magnification objective that could be utilized without compromising the clarity and resolution of the immunostained region under analysis. However, this magnification required that each coronal section of the NL be divided into multiple sample frames for analysis. These data were then compiled to determine the proportional area of NL occupied by 192-IgG immunopositive cells within a given animal and within a given experimental group. All data were downloaded directly into a spreadsheet program (Quatro Pro) for statistical analysis.

#### SON Cellular Morphometry

Morphometric measures of somata and their respective nuclear were collected from the SON contralateral to the knife cut. The purpose of these measures was to investigate the possibility of a differential response between the vasopressin-neurophysin and oxytocin immunoreactive neuronal populations. Previous measures had shown a close correlation between somata and cell nuclear hypertrophy (Watt and Paden, 1992). Therefore, nuclear measures were again collected as a means of providing evidence of enhanced neuronal activity and verification of the somata measures.

The criteria for cell selection was that a distinct cell boundary, a clearly defined nuclear envelope and a prominent nucleolus all be present. Measures were collected by first projecting a microscopic image of the cells of the contralateral SON onto a ZIDAS digitizing pad via an Olympus drawing tube. First, the periphery of the cell body was traced using a stylus interfaced with the digitizing pad. The nucleus was then measured and the cross sectional area of each measure was then

automatically printed. All measures collected were then loaded into a spreadsheet program (Quatro Pro) for analysis. Mean cross sectional area of cell bodies and nuclei were then calculated for each animal and each experimental time point.

#### Glial Morphometry

Morphometric measures of pituicyte nuclei numbers and cross sectional area were collected from one micron thick sections of Spurr's-embedded NL. Pituicyte nuclei have previously been reported to undergo a mitotic and hypertrophic response during periods of increased neurosecretory activity induced by dehydration (Krsulovic and Bruckner, 1969). The purpose of these measures was to determine if pituicyte nuclei may also enlarge during degeneration or axonal sprouting in the partially denervated NL. Such a response would indicate heightened pituicyte activity and provide indirect evidence of pituicyte involvement in the response to partial denervation. Measures were collected by first projecting a microscopic image of a coronal section of the NL onto a ZIDAS digitizing pad via a drawing tube. Sample fields were selected in each of three NL coronal sections per animal by carefully aligning a grid containing five evenly spaced squares along the long axis of the tissue section. The grid was placed on the ZIDAS and observed overlying the section via the drawing tube. Each square corresponded to one  $.02 \text{ mm}^2$  sample field as viewed through a 100X oil objective. At 10X each respective sample field was centered within the viewing field and the 100X objective then engaged. A blank paper was then placed on the ZIDAS overlying the grid and each nuclear profile counted was checked off with either a black (pituicyte) or red (perivascular cell) felt tip pen, thereby ensuring that no nuclei would be counted more than once. This also served to provide a permanent record of all cell counts. The cross sectional area of each NL coronal section sampled was then measured and the mean number of nuclei per unit

area then determined for each section, animal and experimental group.

Measures of pituicyte nuclear cross sectional area were collected by tracing the boundary of each pituicyte nuclear envelope within the sample field that was clearly defined and contained a prominent nucleolus. All measures were then loaded into a spreadsheet (Quatro Pro) for analysis. The luminal surface of every blood vessel displaying a clearly defined endothelial wall within each of the five sample fields was traced in a like manner. Again, these data were then loaded into a spreadsheet for analysis.

#### Metabolic Analysis

A total of 12 lesion animals and 6 sham control animals were individually housed in Nalgene metabolic cages throughout the 100 day experimental period. Daily drinking and urine excretion volumes were determined directly from graduated drinking and urine collection tubes, respectively. Urine samples were collected at a consistent time every day (10:00 am) by pulling off a 2.0 ml sample from a consistent sample depth and the sample was briefly centrifuged at low speed to remove any precipitation or food contaminants prior to analysis. A 10.0 ul sample was then applied to a vapor pressure osmometer (Wescor) to determine the relative urine osmolality for each animal every day. Baseline data on urine excretion volume, daily drinking volume and urine osmolality were established over a seven day period prior to surgery. This period ensured the subject animal's adjustment to the metabolic cage as well as the daily sample collection and cage cleaning routine.

#### Statistical Analysis

One way analysis of variance was performed using the MSUSTAT AV1W program (developed by Dr. R.D. Lund). ANOVA was followed by testing the significance of differences in group means using the MSUSTAT program COMPARE and the Neuman-Keuls and Least Significance Difference test.

## RESULTS

Post-Mortem Observations within the Hypothalamus

The efficacy of the hypothalamic knife cut was determined by examining brain sections stained with cresyl violet which were selected from the most rostral to the most caudal aspect of the lesion tract in every animal. Only those animals which sustained a complete unilateral transection of the hypothalamo-neurohypophysial tract were included in any subsequent investigation. The knife cut was often accompanied by a marked edema and cerebral hemorrhage resulting in varying degrees of cavitation surrounding the knife path. This cavitation extended from the dorsal surface to varying depths of the brain in most lesion animals, particularly at early post-lesion times, and to a lesser extent in sham controls. The cavitation typically compressed the ipsilateral PVN, resulting in complete neuronal death. Rarely were any ipsilateral PVN neurons spared. No apparent displacement of the contralateral PVN or ipsilateral SON was ever observed. Within the cavity of the lesion tract was an extensive invasion of macrophages, monocytes and other blood born elements which persisted throughout the first 10 days following surgery. Within the parenchyma surrounding the knife cut an extensive gliosis was consistently observed which persisted for the first two weeks post-lesion. A marked hypertrophy of astrocytes was apparent throughout the ipsilateral hemisphere and particularly in close proximity to the lesion tract. No such astrocyte hypertrophy was notable in the contralateral hemisphere except within the corpus callosum.

Neovascular growth was observed surrounding the knife tract in all animals as early as 10 days following the knife cut with new vessels developing in close juxtaposition to the lesion wall. These vessels ranged in size from small arterioles to vessels with diameters greater than any observed within the hypothalamus of the normal animal. In a

serendipitous observation it was noted that by 90 days following the knife cut much of the neovasculature surrounding the lesion tract was selectively immunostained, using silver-enhanced immunogold labeling, with antibodies against the neuropeptide oxytocin-neurophysin. However, when adjacent sections were prepared in an identical fashion with antibodies against vasopressin-neurophysin, no immunostaining was ever observed (Fig. 1). This observation was made in animals of both the 30 and 90 day PS groups across literally dozens of like preparations. Immunostaining was never observed in any tissues prior to 30 days PS,

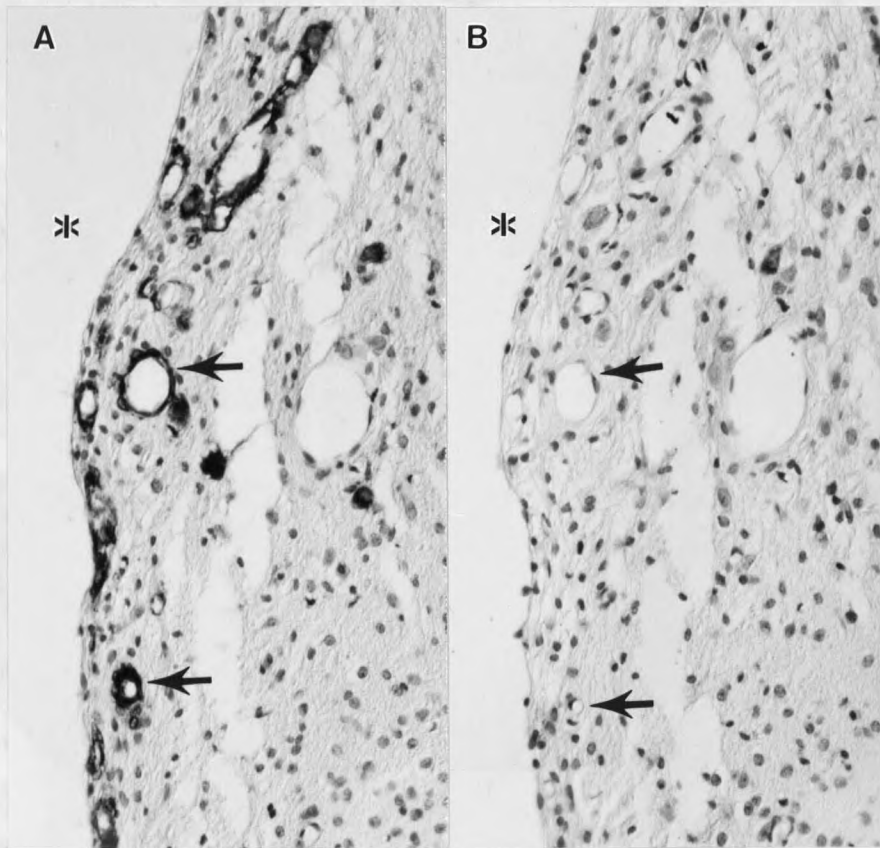


Figure 1. Oxytocinergic Perivascular Plexus Within the Hypothalamus. A. Silver-enhanced immunogold localization of oxytocin-neurophysin immunoreactive plexus surrounding the neovasculature in the 90 day animal (solid arrows). B. An adjacent section stained with vasopressin-neurophysin in an identical fashion (solid arrows). A linear scar forms the boundary of the lesion tract (asterisk). Magnification, 200X.

nor were individual axons or fiber bundles observed coursing toward these apparent neurosecretory plexuses. However, fibers were observed projecting between individual plexuses in close juxtaposition to the cavity wall. Perivascular plexuses were observed in animals regardless of the extent of neuronal loss in the ipsilateral SON. The possibility of non-specific staining seems remote given that the internal surface of the lesion cavity and tears within the tissue show no immunoreactivity. Likewise, many vessel profiles were observed throughout the brain which showed negative immunoreactivity.

The specificity of staining for oxytocin vs vasopressin-neurophysin peptides, the appearance of immunopositive plexuses at only 30 and 90 days PS and the absence of non-specific staining suggest that the plexuses form through extensive outgrowth of hypothalamic neurosecretory axons.

#### Lesion-Induced Changes in Urine Osmolality, Excretion, and Daily Water Intake.

The principle objective of this experiment was to determine if the stimulus for the compensatory axonal sprouting observed was due to a response by the neurosecretory system to recover from a functional deficit in circulating plasma VP levels or to a growth response due in part to lesion-induced stimuli. The first step in exploring these possibilities was to determine if, in fact, the antidiuretic system had been compromised by the lesion.

The possibility of lesion-induced changes in circulating plasma VP levels was explored indirectly by measuring urine osmolality as well as daily drinking and urine excretion volumes. Daily measurements of urine osmolality revealed an initial transient hypoosmolality, followed within 48 hours by a chronic and significant ( $P < .05$ , t-test,  $t = 1.76$ ,  $n = 79$ ) hyperosmolality which persisted throughout the 90 day post-surgical survival period (Fig. 2). The occurrence of the transient hypoosmolality would suggest a substantial decrease in plasma VP levels

immediately following surgery which occurred in spite of a concomitant decrease in both water intake and urine excretion volumes. The transient rebound in urine osmolality which occurred from day 2 to day 5 PS may reflect either a compensatory over-responsiveness resulting in heightened secretion of plasma vasopressin or release of VP stores from degenerating terminals. The urine osmolality then stabilized at a level significantly above that of sham control values for the remainder of the experimental period.

A chronic and significant ( $P < .05$ ,  $t$ -test,  $t = 1.78$ ,  $n = 79$ ) decrease in both daily water intake (Fig. 3) and urine excretion volumes (Fig. 4)

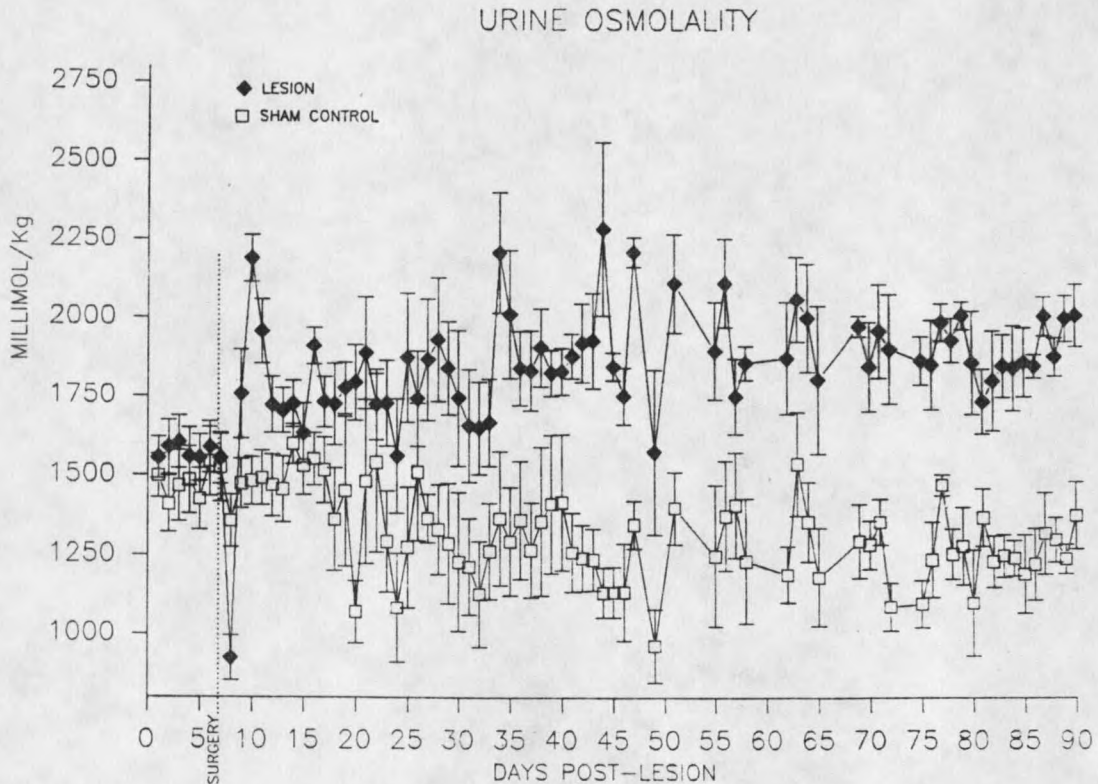


Figure 2. Effects of unilateral hypothalamic lesion on urine osmolality. Urine osmolality decreased markedly within the first 24 hours following surgery and then immediately increased to a significantly ( $P < .05$ ) hyperosmotic state which persisted throughout the experimental period.

began immediately following surgery and persisted throughout the post-surgical period, paralleling the increased urine osmolality. These data suggest that the lesion did not result in a functional deficit in circulating VP levels.

Hypertrophy of SON Somata and Nuclei Following Partial Denervation.

Cellular hypertrophy within the magnocellular neurosecretory system occurs following experimental induction of heightened metabolic activity via salt loading (Paterson and Leblond, 1977) or dehydration and lactation (Watson, 1965) and is an accepted indicator of heightened cellular activity (Vogels et al., 1990).

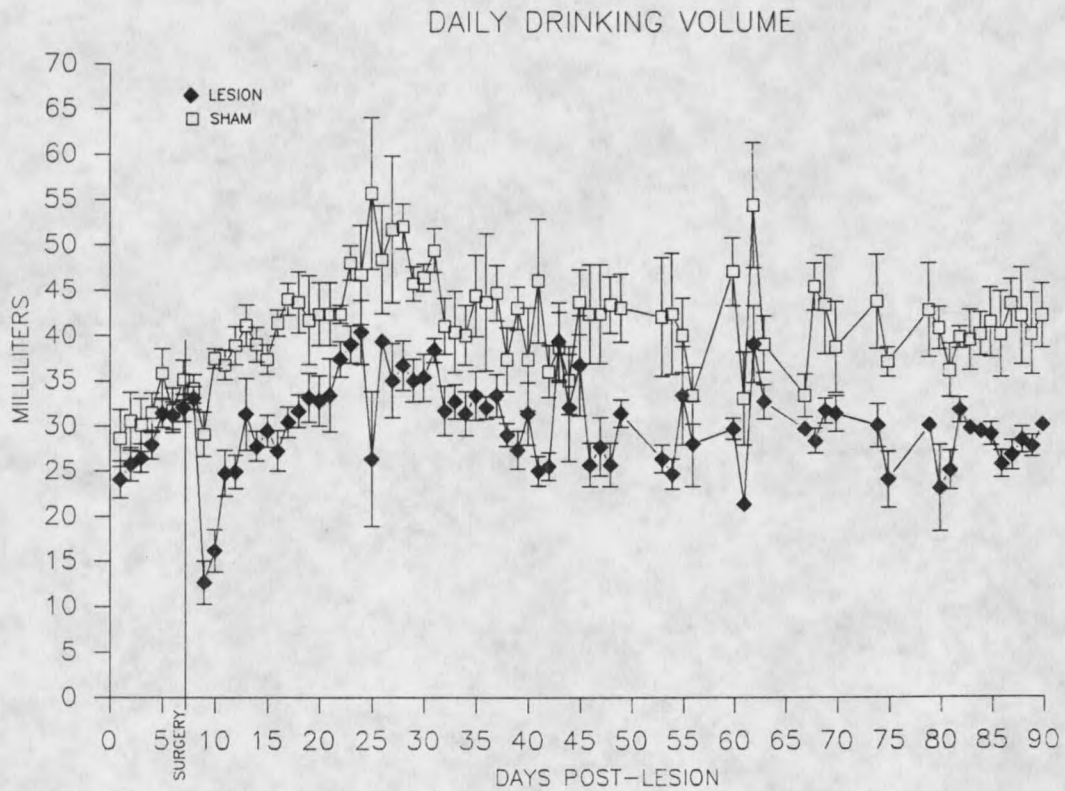


Figure 3. Effects of unilateral hypothalamic lesion on daily drinking volume. Daily water intake was significantly ( $P < .05$ ) reduced within 24 hours of the surgical intervention and remained depressed throughout the experimental period.

Furthermore, cellular hypertrophy following partial denervation of a terminal field has been correlated with axonal sprouting contralateral to the site of injury (Goldschmidt and Steward, 1980). In a previous investigation (Watt and Paden, 1991) an enlargement of both magnocellular somata and their respective cell nuclei was demonstrated in the contralateral SON and PVN following partial denervation of the NL. Furthermore, these data indicated the hypertrophy occurred during the sprouting phase of the post-lesion response. However, the histochemical staining paradigm used did not distinguish between oxytocin and vasopressin magnocellular neurons, the two cell types in the nucleus (Fig. 5).

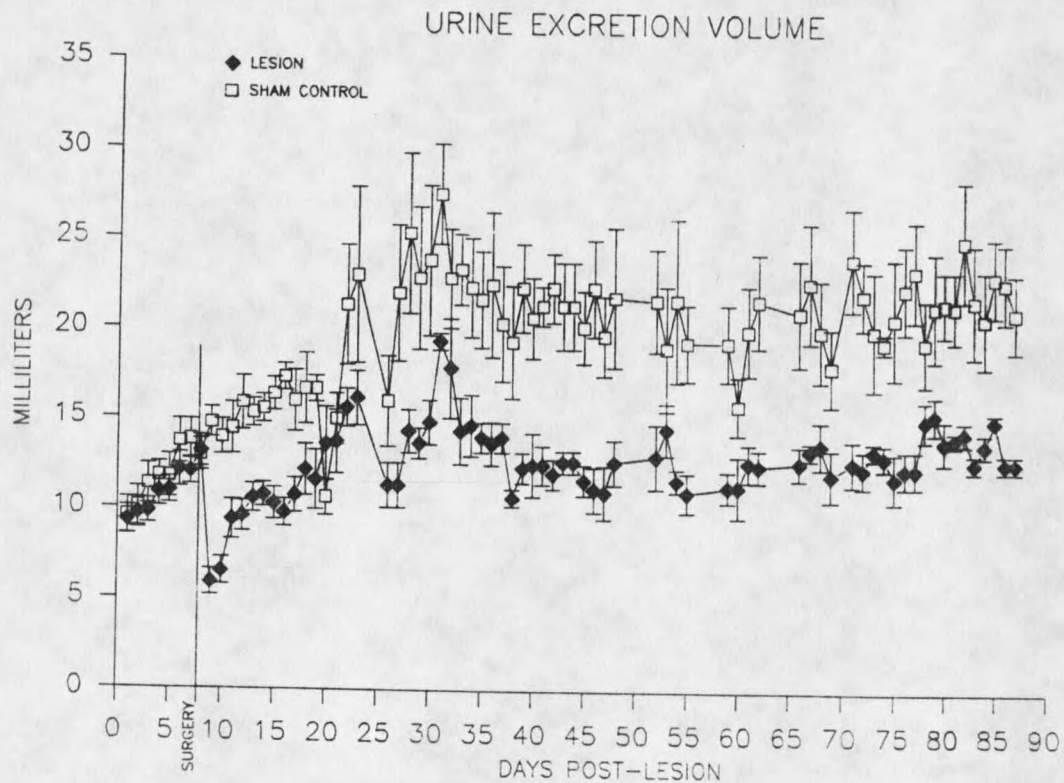


Figure 4. Effects of unilateral hypothalamic lesion on daily urine excretion volume. Daily urine excretion volume was significantly ( $P < .05$ ) reduced within 24 hours of the surgical intervention and remained depressed throughout the experimental period.

These distinct cell populations display differences in the temporal pattern of axonal outgrowth and penetration of the NL terminal field during development. It seemed reasonable then to explore the possibility of a differential hypertrophic response between the vasopressin and oxytocin immunoreactive neurons within the contralateral SON following partial denervation of the NL. A highly significant enlargement of vasopressin immunoreactive neurons ( $F=12.6$ ,  $P<.00001$ , one way ANOVA,  $df=6/29$ ) and nuclei ( $F=8.67$ ,  $P<.00001$ , one way ANOVA,  $df=6/30$ ) occurred following surgery when compared to controls.

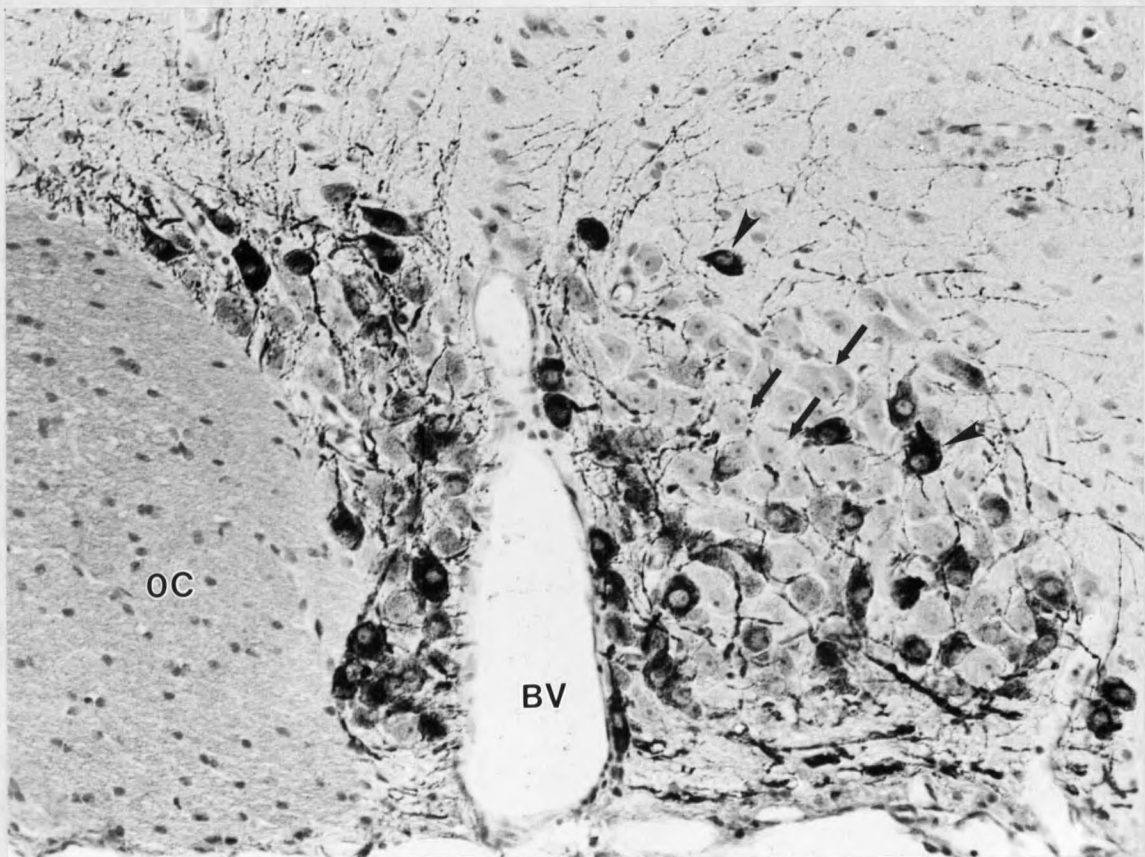


Figure 5. Photomicrograph Demonstrating Silver-Enhanced Oxytocinergic SON Neurons. Demonstration of the silver-enhanced immunogold labeling of oxytocinergic magnocellular neurons in the SON utilizing anti synthetic-oxytocin antibodies (solid arrowheads). The non-immunolabeled cells are vasopressinergic magnocellular neurons (arrows). Note the numerous immunolabeled fibers within and dorsal to the nucleus. (OC) Optic chiasm, (BV) blood vessel. Magnification, 100X

By 10 days PS there was a 12% increase (one way ANOVA, Neuman-Keuls post hoc comparison, not statistically significant (NS)) in the cross sectional area of vasopressin-immunoreactive somata over age-matched control values (Fig. 6). By 30 days PS the difference had increased to 23.7% ( $P < .01$ , Neuman-Keuls) followed by a return to a 12% enlargement above age-matched intact control values by 90 days post lesion (NS). Within the control groups a continued growth of the vasopressin somata was evident throughout the experimental period. A significant 27% ( $P < .01$ , Neuman-Keuls) increase in somata size was apparent between the lesion day 0 and 90 day PS control.

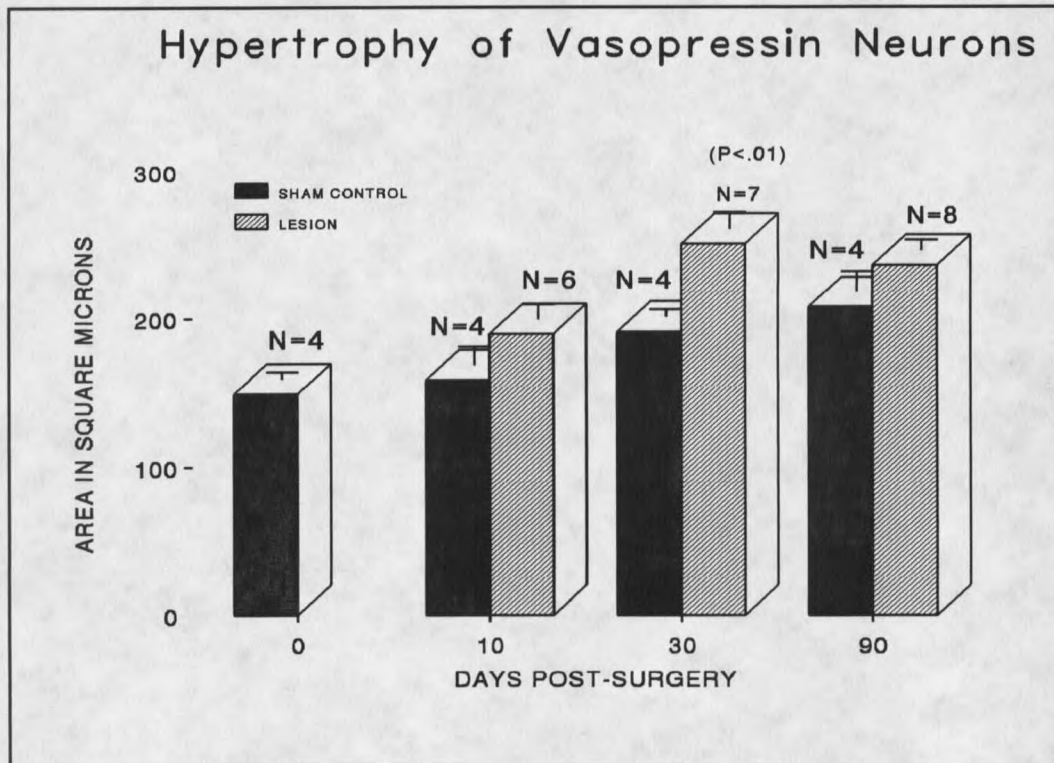


Figure 6. Hypertrophy of Vasopressinergic Neurons. The cross-sectional areas of at least 25 vasopressin magnocellular neurons were measured in the contralateral SON nucleus of each animal. Age-matched sham controls were included at 10, 30 and 90 days post-surgery. Somata were hypertrophic by 10 days, had reached significantly larger areas than controls by 30 days and remained enlarged throughout the post-surgical period. Note the continued enlargement of somata with age in control animals.

This continued cellular growth beyond the first 35 days post-parturition demonstrates the importance of including age-matched controls in these experiments. The nuclei of these same VP-IR neurons reflected a similar, albeit not identical, pattern (Fig. 6). At 10 days PS there is a non-significant but readily apparent 12.7% decrease in the lesion group nuclear cross-sectional area when compared to age-matched control values. However, by 30 days PS a significant ( $P < .01$ , Neuman-Keuls) increase in cross sectional area became evident with nuclear area 20% above age-matched control values. By 90 days PS the nuclear enlargement was no longer significantly different from

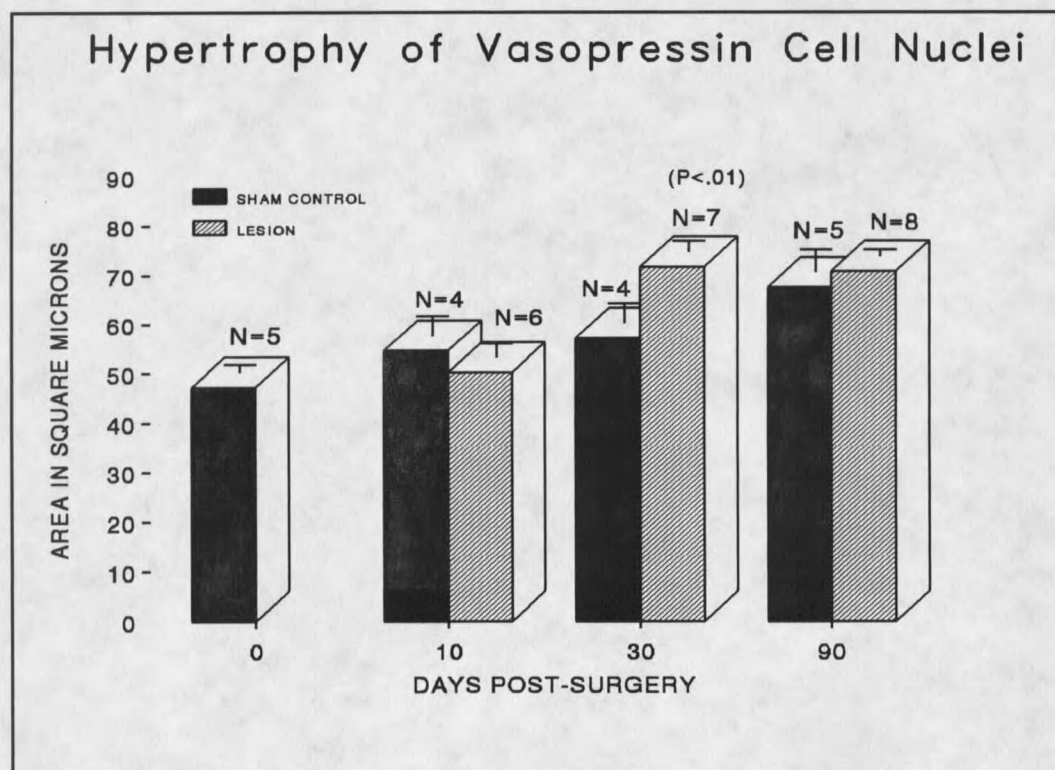


Figure 7. Hypertrophy of Nuclei in Vasopressinergic Neurons. The cross-sectional areas of at least 25 vasopressin magnocellular cell nuclei were measured in the contralateral SON of each animal. Age-matched sham controls were included at 10, 30 and 90 days post-surgery. A significant hypertrophy of somata occurred by 30 days ( $P < .01$ ), which then returned to values no different from age-matched controls by 90 days PS.

age-matched control values. Thus, VP cellular nuclei demonstrate a more temporally restricted response than observed in VP somata. A continuing age related enlargement in nuclear cross sectional area was also apparent in the control groups reflected by a significant 28% ( $P < .01$ , Neuman-Keuls) increase between day 0 and 90 days PS.

A highly significant enlargement of OT-immunoreactive somata ( $F=9.24$ ,  $P < .00001$ , one way ANOVA,  $df=6/28$ ) and cell nuclei ( $F=6.6$ ,  $P < .0002$ , one way ANOVA,  $df=6/29$ ) was also observed (Fig. 7). By 10 days PS a robust enlargement of OT somata was evident with mean cell

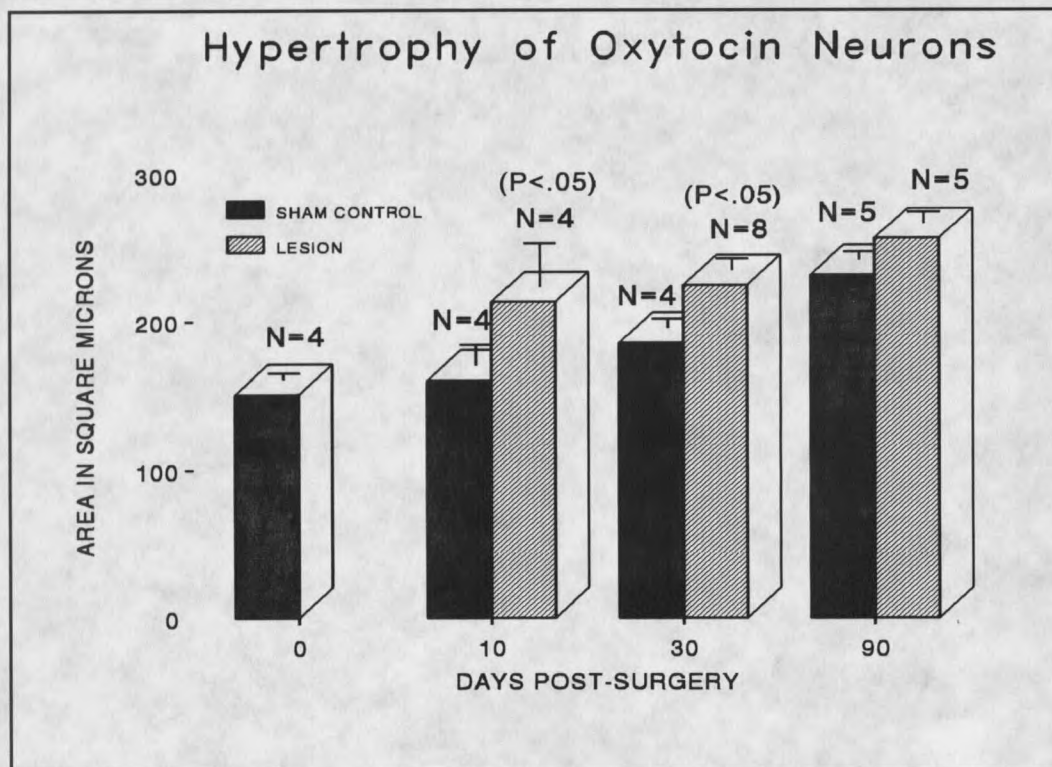


Figure 8. Hypertrophy of Oxytocinergic Neurons. The cross-sectional areas of at least 25 oxytocin magnocellular neurons were measured in the contralateral SON nucleus of each animal. Age-matched sham controls were included at 10, 30 and 90 days post-surgery. A significant hypertrophy of somata occurred by 30 days ( $P < .01$ ), which then returned to values no different from age-matched controls by 90 days PS.

cross sectional area 24.7% above the age-matched control value. This difference was maintained throughout the experimental period, with experimental values 17% and 9.8% above age-matched control values at 30 and 90 days post-lesion, respectively. Average nuclear cross sectional areas were also markedly enlarged (NS) by 10 days PS reaching 19% above age-matched control levels (Fig. 8). This difference was maintained at 17.4% at 30 days PS but had disappeared by 90 days PS. Enlargement of somata and cell nuclei was also evident in the control tissues reflecting a continuing growth process in these cells throughout the experimental period.

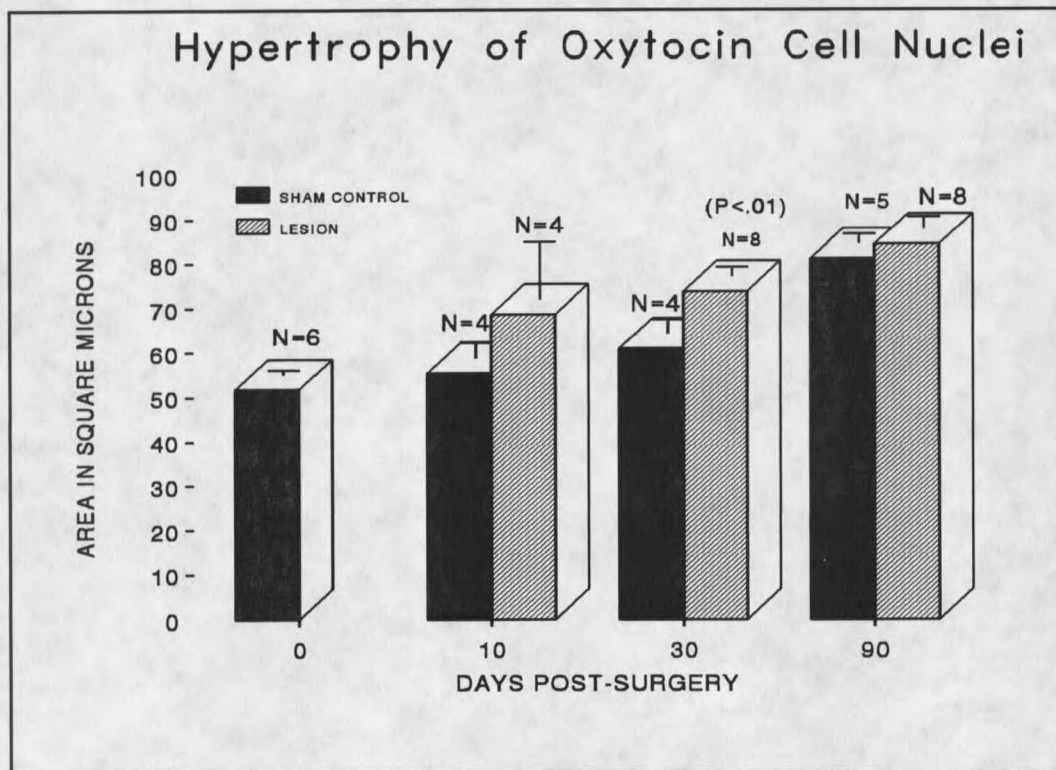


Figure 9. Hypertrophy of Nuclei in Oxytocinergic Neurons. The cross-sectional areas of at least 25 oxytocinergic magnocellular cell nuclei were measured in the contralateral SON of each animal. Age-matched sham controls were included at 10, 30 and 90 days post-surgery. A marked enlargement was apparent by 10 days PS persisting at 30 days, and disappearing by 90 days PS.

Although both the vasopressin and oxytocin immunoreactive neurons undergo a lesion-induced hypertrophy there are indications that the oxytocinergic neurons and their respective nuclei may respond more rapidly and/or more vigorously than their vasopressinergic counterparts.

Morphometric Assessment of the Neural Lobe Vascular Plexus.

Vascular endothelial cells show little proliferative activity in the mature animal (D'Amore and Thompson, 1987) indicating a low rate of collateral vessel growth under normal conditions. However, under certain conditions these normally quiescent cells may exhibit considerable growth. Formation of the corpus luteum, chronically exercised muscle, psoriasis, atherosclerosis, arthritis, tumor vascularization and wound healing are all conditions which promote or require vascular growth. In the neurosecretory system an extensive collateral vessel ingrowth has been demonstrated in the relatively avascular proximal infundibulum following hypophysectomy (Raisman, 1973; Adams, et al, 1969; Beck, et al, 1969). Furthermore, the neovascular sprouting precedes that of the regenerative sprouting of the neurosecretory axons. It has been suggested that this vascular growth may act as a stimulus for the subsequent regenerative axonal sprouting (Raisman, 1973). Given this possible link between neovascular sprouting and neurosecretory axonal sprouting, a morphometric investigation of the vascular network within the partially denervated NL was undertaken in an effort to further elucidate the mechanisms involved in the initiation or maintenance of compensatory sprouting in the NL.

Figure 10 illustrates the mean number of vessel profiles/mm<sup>2</sup> within the NL of lesion and age-matched intact control animals. Although development of the NL vascular plexus is thought to reach maturity by 20 days of age in the mouse (Eurenius, 1977) and 30 days in the rat (Galabov and Schiebler, 1983) these data indicate a continued increase in capillary profiles until at least 45 days of age (PS 10).

The number of vessel profiles/unit area then shows a downward trend reflecting an age-related reduction in vessel numbers or an increase in NL area continuing to at least 90 days PS. In contrast, the lesion groups show a slight increase in vessel density by 2 days PS which continues for at least 90 days reaching levels significantly higher ( $P < .01$ , Neuman-Keuls) than age-matched control values at 90 days (Fig. 10). It seems likely that these data reflect the maintenance of the early postnatal vessel density as opposed to a lesion-induced collateral sprouting of NL vessels. The difference observed in vessel densities between 90 day lesion (Fig. 11a) and age-matched controls

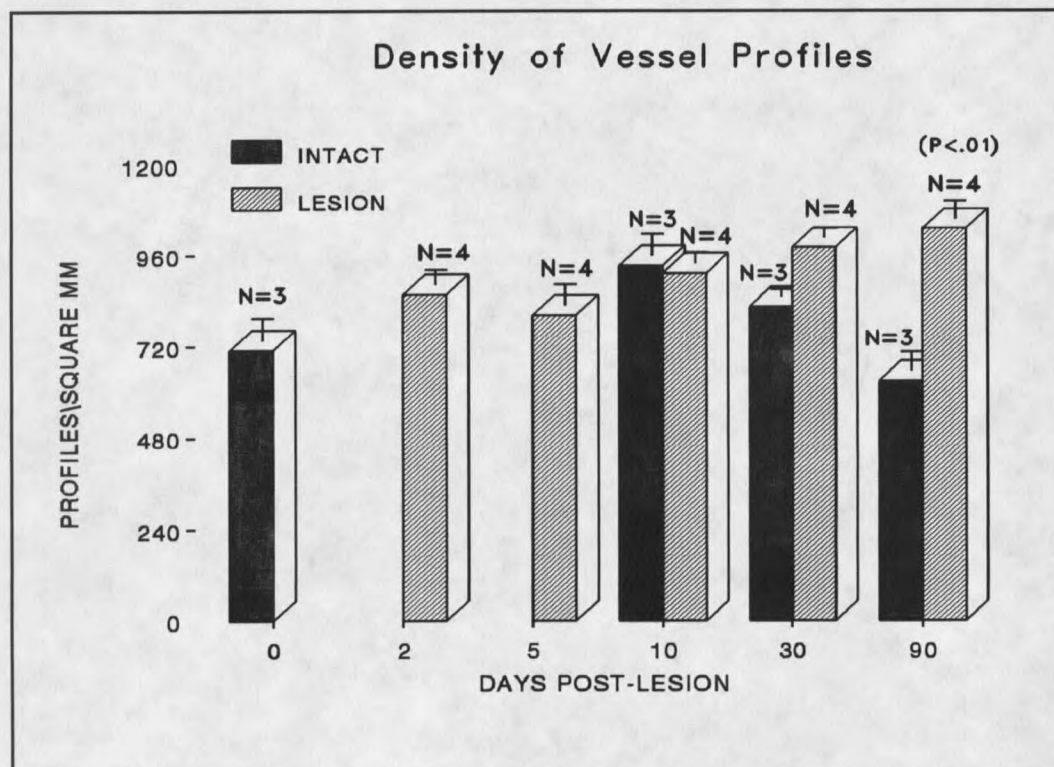


Figure 10. Effects of lesion on blood vessel density in the NL. A gradual increase in vessel density occurred throughout the post-surgical period. There was a concomitant age-related decline in the vessel density in control animals which resulted in a significant difference in vessel density by 90 days PS.

(Fig. 11b) was readily apparent. In order to further explore this possibility the size of the vessels within each experimental group was sorted by cross-sectional area into 1 of 10 bins (Table 1). The rationale for this approach was that an increase due to endothelial proliferation would be evident as a relative increase in the number of small vessels, i.e. capillaries, as opposed to the larger arterioles and venuoles.

Table 1. Size Distribution Bins of NL Vascular Morphometry

Bin #	Vessel Area		Equivalent Circle	
	Range ( $\mu\text{m}^2$ )	Mean ( $\mu\text{m}^2$ )	diameter( $\mu\text{m}$ )	perimeter( $\mu\text{m}$ )
1	.933-1.33	1.13	1.20	3.77
2	1.34-5.34	3.33	2.06	6.47
3	5.35-9.34	7.33	3.05	9.60
4	9.35-13.4	11.35	3.80	11.94
5	13.5-33.4	23.37	5.45	17.14
6	33.5-53.4	43.38	7.43	23.35
7	53.5-93.4	73.38	9.67	30.37
8	93.5-134	113.39	12.02	37.75
9	134-540	340.00	20.81	65.36
10	541-941	741.00	30.72	96.50

Examination of the PS 2 lesion group indicates little difference in the number of small vessels, when compared to day 35 intact controls. However, there is a marked increase in the number of larger vessels (bins 6-9) which may be indicative of an acute vasodilatory response (Fig. 12). By PS 5 these differences in distribution of vessel size are still apparent although to a less pronounced degree, consistent with indications of an early, acute vasodilatory response.

By 10 days PS a marked increase in the number a smaller vessels becomes apparent. By 30 days the continued increase in vessel numbers now extends to include all size distribution bins (data not shown). This trend is best illustrated at 90 days PS where increased vessels were observed in all size categories (Fig. 13). In summary, the increase in large diameter vessels at 2 and 5 days PS with no comparable increase in the number of small vessels indicates a vasodilatory

response. This is followed at 10 days PS by a slight increase in the number of small vessels which continues at 30 and 90 days PS. By 90 days PS however, a shift to increased numbers of large vessels is apparent as well.

By 125 days of age (PS 90) a distinct pattern becomes evident. Vessel numbers drop off markedly from earlier age groups in bins 3-5 while remaining essentially equal in bins 7-10. These data indicate an age-related reduction in the number of small vessels with no equivalent reduction in the largest vessels measured (Fig. 11).

These data indicate either growth of new collateral vessels or the maintenance of the early postnatal vascular plexus over a period when, in the normal animal, a decline in the number of small vessels is apparent.

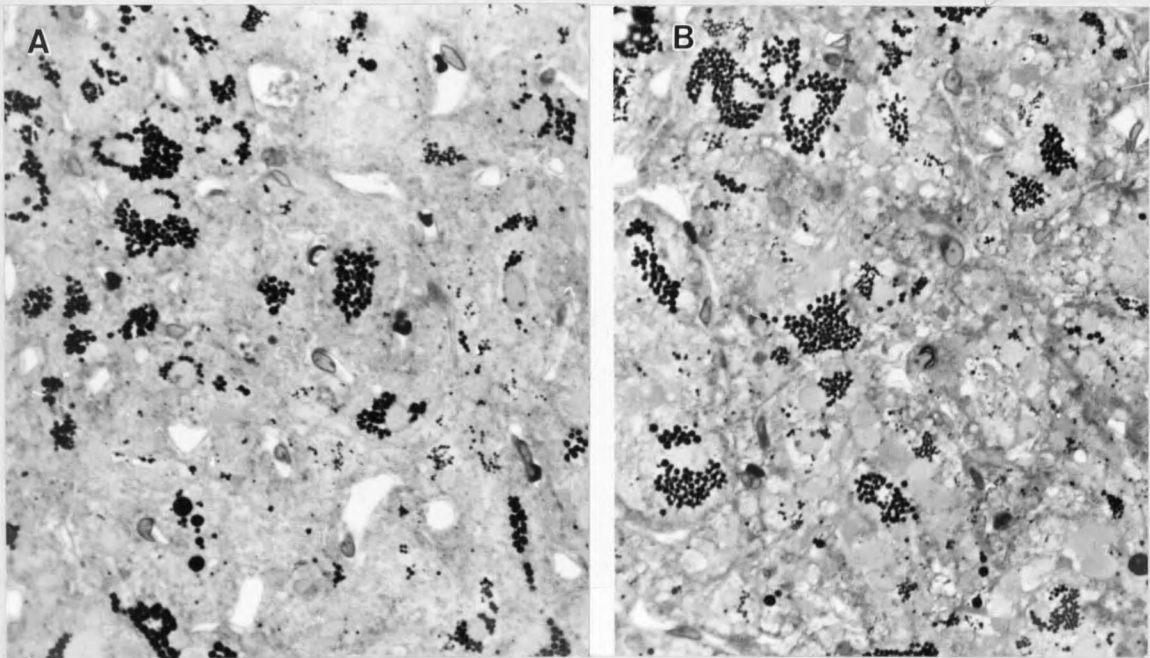


Figure 11. Photomicrograph of NL Vasculature. Higher density of blood vessels is maintained following unilateral knife cut. A. Neural lobe of the lesion animal at 90 days PS. Note the large number of small vessels perforating the NL. B. Neural lobe of age-matched intact control tissue demonstrating the relative absence of blood vessels. Magnification, 1000X.

The proportional area of the sample fields occupied by vessel lumen was calculated to determine the net effect of the change in vessel numbers on proportional vascular area (Fig. 14). These data indicate a significant ( $P < .01$ , Neuman-Keuls) increase in the proportional area of the NL occupied by vascular elements within 48 hours PS when compared to lesion day 0 controls. By 5 days PS the response had waned with no further differences between lesion and control animals observed. However, from 30-90 days PS an upward trend in vessel number/unit area became apparent in all size distribution bins (see Fig. 11). Why then would this increase not be evident in the proportional area analysis?

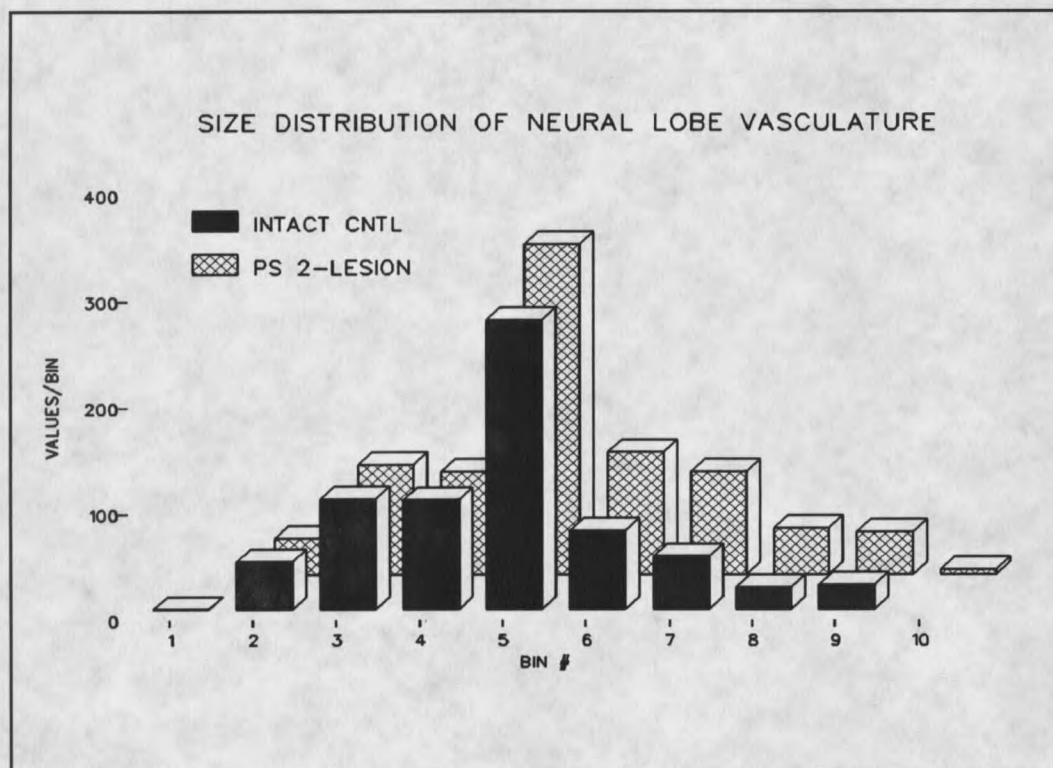


Figure 12. Size Distribution of PS 2 Neural Lobe Vasculature. Increased vessel profiles were observed in the largest bin size categories reflecting a vasodilation response 2 days following partial denervation.

As a means of reapproaching this apparent discrepancy the proportional areas were again plotted but excluding bins 8, 9, and 10 (Fig. 15). The largest vessels, presumably arterioles and venuoles, by their very size could mask any increase in proportional area resulting from an increase in the size of the capillary plexus. These results demonstrate a pattern essentially identical to those displayed in Figure 10. The increase in proportional area observed at 2 days PS has returned to levels more representative of the vessel density observed at the same time, while by 90 days PS the proportional area of the lesion group is significantly higher ( $P < .05$ , Neuman-Keuls) than intact controls.

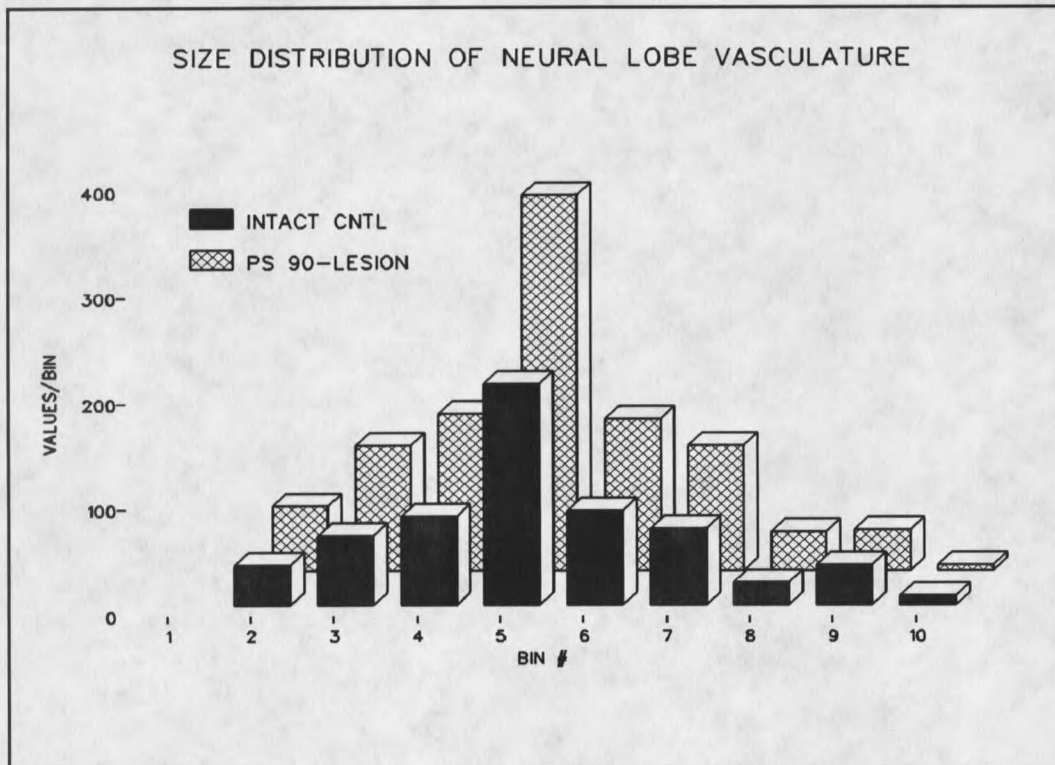


Figure 13. Size Distribution of PS 90 Neural Lobe Vasculature. Increased vessel profiles were observed in all size categories at 90 days PS reflecting the absence of an age-related decline in vessel density apparent in control tissues.

These values now appear to more accurately reflect the observed increase in vessel density. Although these data do not necessarily reflect a growth response per se they do indicate that the principle alteration of the NL vasculature was in the capillary plexus as opposed to the larger arterioles and venules.

Low Affinity (p75) Nerve Growth Factor Receptor Immunoreactivity in NL.

Monoclonal antibody (Mab) IgG-192 has been shown to bind specifically to low affinity nerve growth factor receptors (NGFR) in intact NL, infundibulum and median eminence but not anterior lobe.

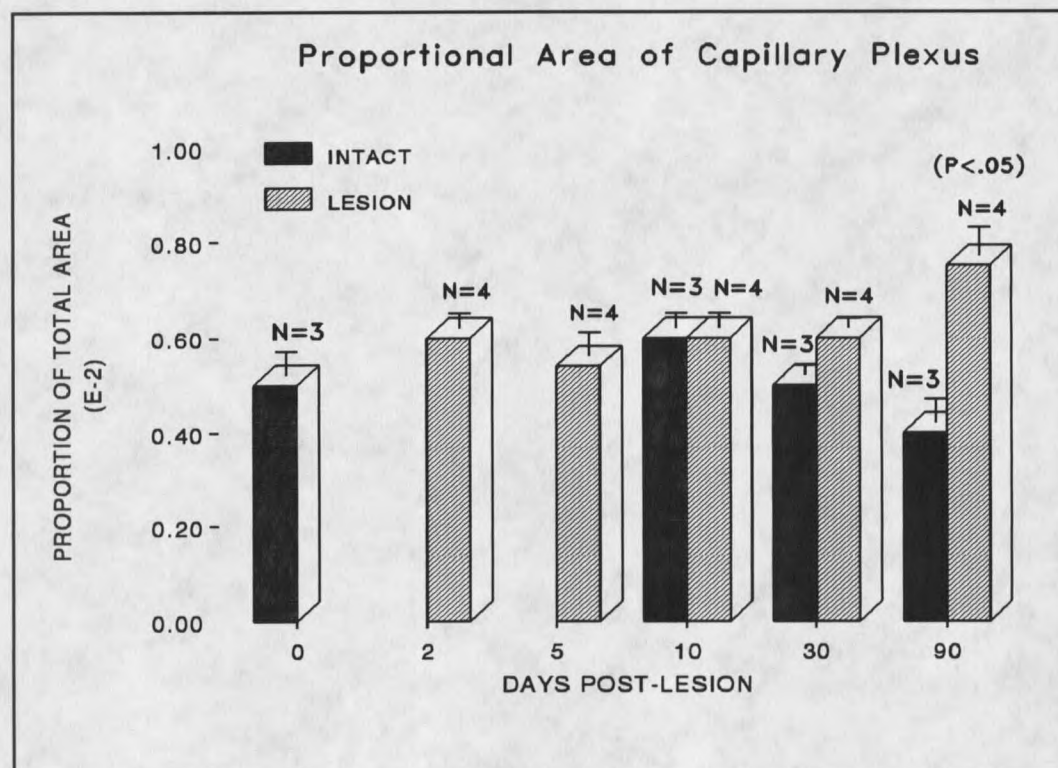


Figure 14. Mean Proportional Area of NL Vasculature. An early, acute increase in the mean proportional area of NL vasculature is evident at 2 days PS ( $P < .01$ ). No further differences were observed between lesion animals and controls.

An up-regulation of NGFR densities has also been demonstrated in neural lobe at 7 and 15 days following infundibular stalk section with the immunopositive cells found predominately, but not always, in the vicinity of capillaries (Yan and Johnson, 1990).

However, the identity of the cells demonstrating this increased expression of NGF receptors has not yet been conclusively determined. Armed with these data, I sought to explore the possible upregulation of NGFR-immunoreactivity (NGFR-IR) in the NL and its possible correlation with degeneration and sprouting.

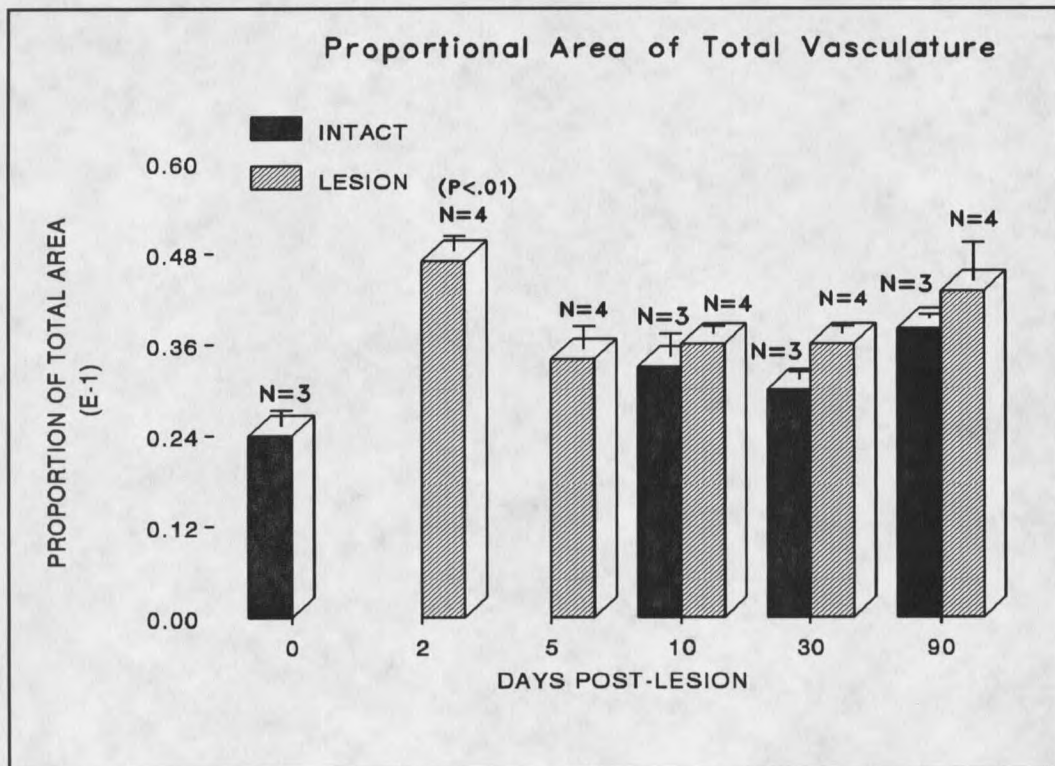


Figure 15. Mean Proportional Area of NL Capillary Plexus. Proportional area analysis of the capillary plexus demonstrates no acute vasodilation at 2 days PS. An age-related decline in capillary area was observed in all control tissues. In contrast, the lesion animals show an increase in the proportional area occupied by capillaries which correlates closely with the increased density of the capillary plexus noted earlier.

Figure 16 illustrates the results of the proportional area analysis of NGFR-IR in the NL. A highly significant increase ( $F=9.8$ ,  $P<.0002$ , one way Anova,  $df=11/59$ ) in the proportional area of NL occupied by NGFR-IR elements occurred following partial denervation.

Two days following surgery no noticeable difference existed between lesion animals and age-matched sham controls. By 5 days PS a significant 70% ( $P<.05$ , least significant difference test (LSD)) increase in the proportional area of NL occupied by NGFR-IR elements had occurred in lesion animals when compared to sham controls (Fig. 17).

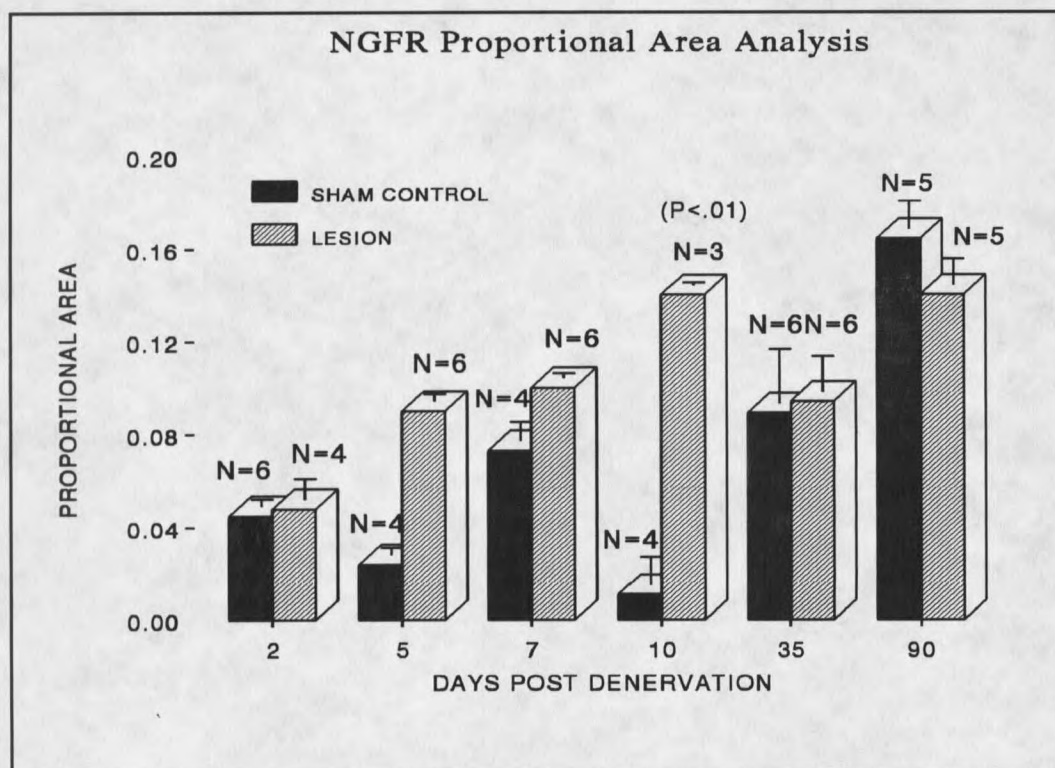


Figure 16. 192-IgG Immunoreactivity in the NL. A significant increase in the proportional area of NL immunoreactive for nerve growth factor receptor was evident within 5 days PS. This trend continued reaching peak values by 10 days PS then returned to normal levels by 30 days PS. An age-related increase in NGFR proportional area is evident as well.

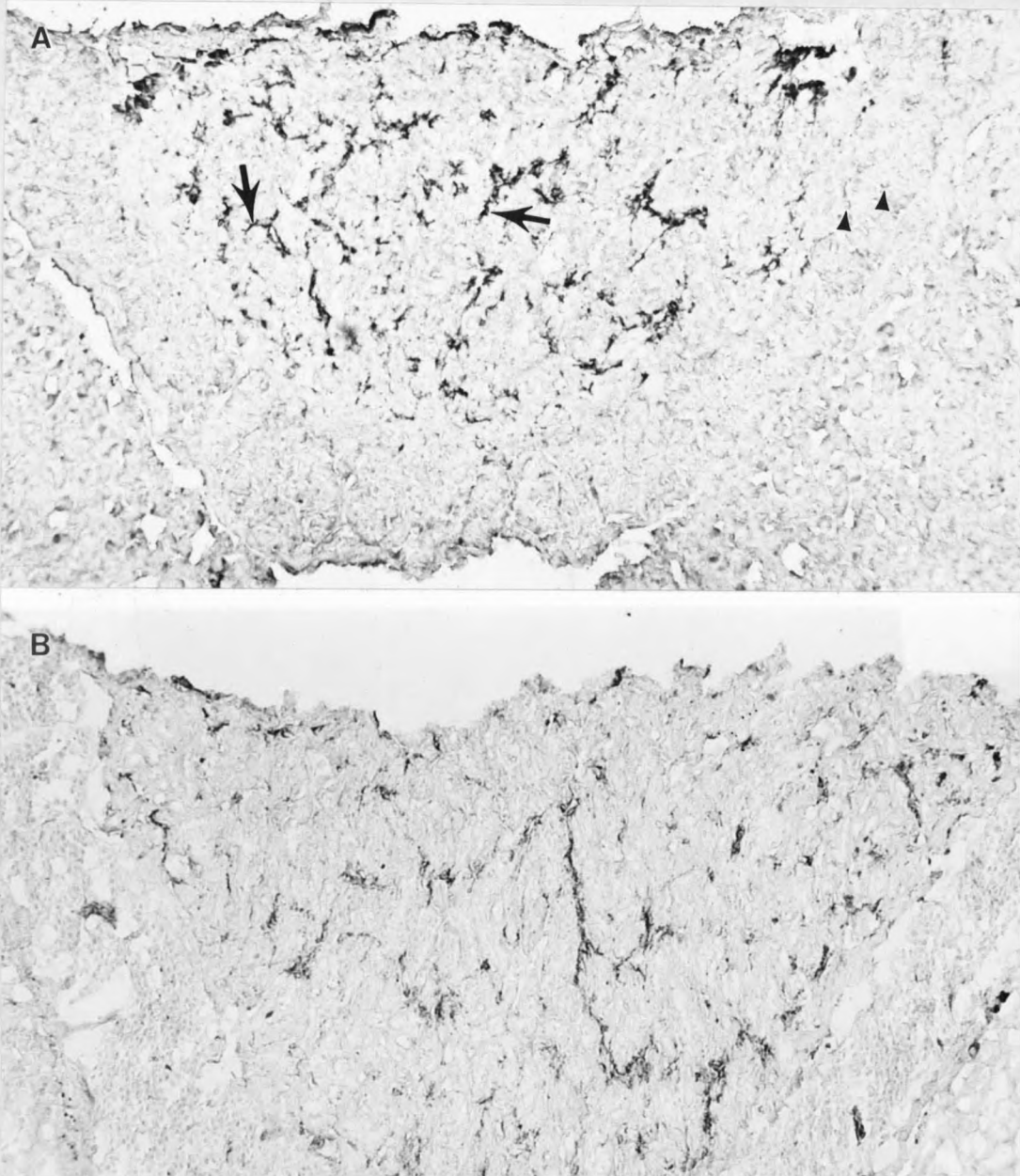


Figure 17. Photomicrograph of NGFR immunoreactivity patterns in the NL at 5 days PS. A) Immunocytochemical application of 192-IgG in 5 day post-lesion animals demonstrates a highly immunoreactive staining pattern surrounding blood vessels and extending outward in long finger-like projections (solid arrows), presumably within the perivascular space. Numerous 192-IgG negative glial cell nuclei are evident throughout the section (solid arrowhead). B) Age-matched sham control tissue demonstrating a reduced intensity 192-IgG immunoreactivity and proportional area. Magnification, 650X

This difference was also significant at 7 days PS ( $P < .01$ , LSD) and at 10 days following surgery. By 35 days following surgery the proportional area of NGFR-IR elements had fallen below those observed at 10 days PS and had returned to levels no longer different from age-matched control values. By 90 days PS NGFR-IR levels had increased over those observed at 35 days PS but were not significantly different from age-matched sham control (Fig. 18). The observed increase in NGFR-IR which was apparent in control tissue reflects a previously reported age-related increase in NGFR-IR in the NL of rats (Yan and Johnson, 1990). What is important to note here is the significant increase in NGFR-IR which occurs between 5 and 10 days following surgery, a time when perivascular cell activation and phagocytic activity is at a maximum (Watt and Paden, 1991). These data suggest that a heightened expression of the p75 low affinity NGF receptor coincides with these cellular events.

The possible expression of NGFR antigens by microglia was further explored immunocytochemically utilizing known microglial markers Mab OX-42 (iC3b receptor; Serotec) and OX-1 (leucocyte common antigen; Serotec). OX-1 antigens are thought to be upregulated in activated microglial cells (Perry and Gordon, 1987). Figure 19 illustrates the staining patterns observed. Mab OX-42 stains microglial cells in close proximity to blood vessels and putative parenchymal microglial cells in a highly specific and localized manner. Individual OX-42 positive microglial cells and their characteristic reticular processes could easily be discerned at the light level. The distribution of these immunolabeled cells was essentially homogeneous with no apparent difference in the staining pattern or relative immunoreactivity between the parenchymal and perivascular compartments. A very similar pattern was characteristic of the OX-1 immunostaining reflecting no differences in the distribution of labeled cells as a result of the activation of a subpopulation of microglial cells.

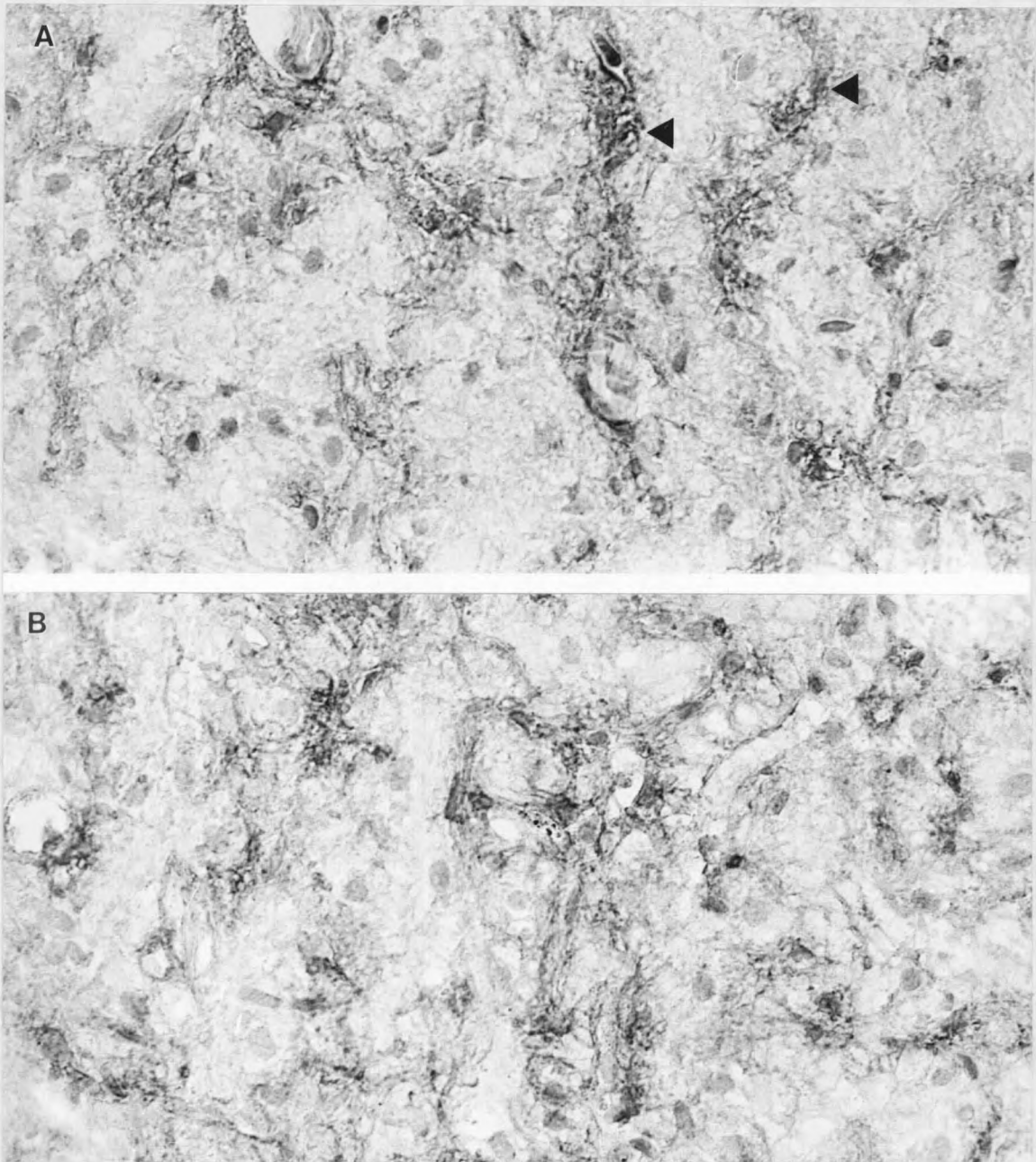


Figure 18. Photomicrograph of NGFR immunoreactivity patterns in the NL at 90 days PS. A. 90 days post-lesion 192-IgG staining intensity (solid arrowheads) is reduced from levels observed at 5 days PS and are no different from age matched sham controls. However the staining pattern and the proportional area of staining are similar to that observed at 10 days PS reflecting an age-related increase in nerve growth factor receptor expression. B. Age-matched sham control tissue. Magnification, 650X.

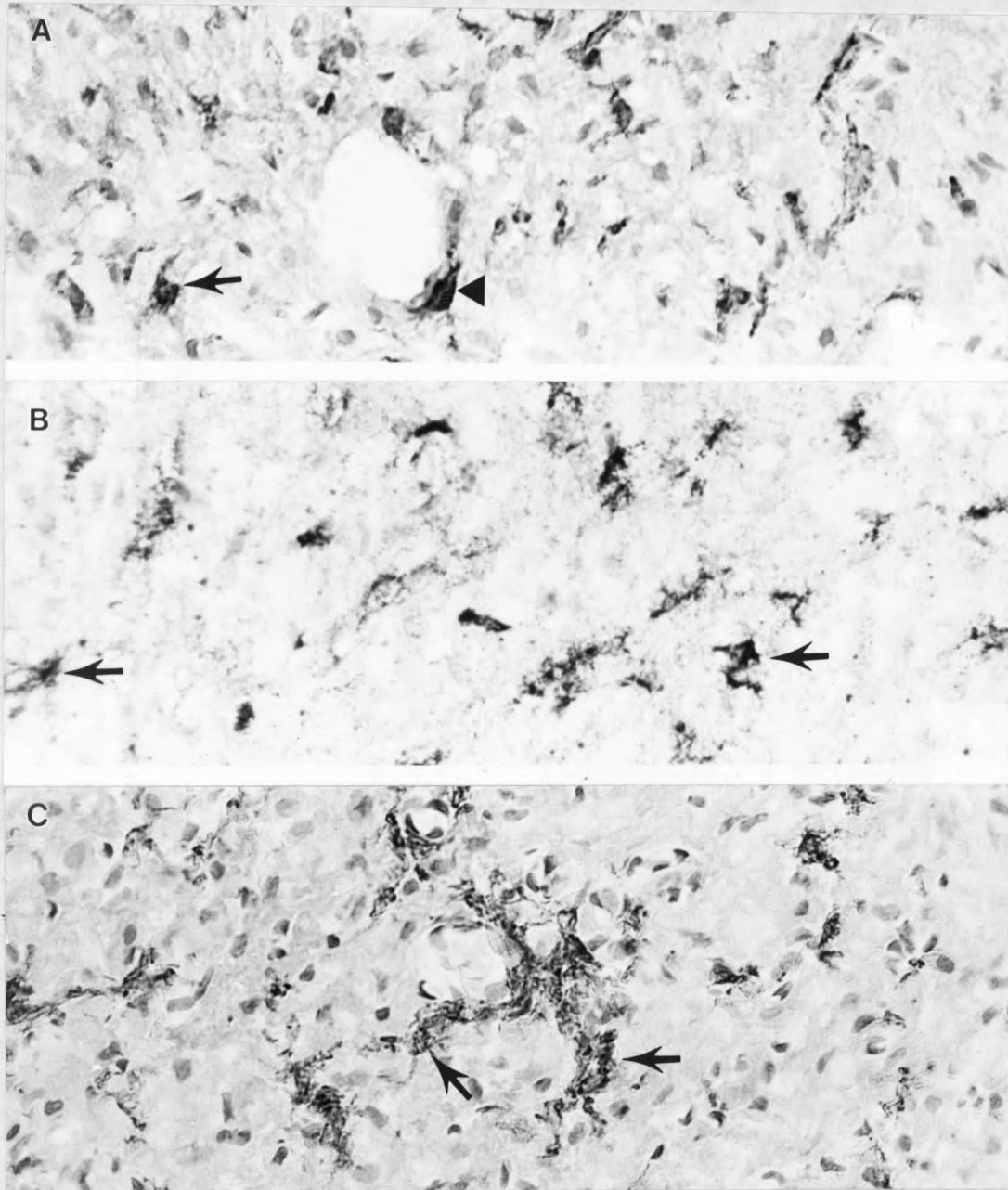


Figure 19. Photomicrograph of microglial cells in the NL at 5 days PS. A. OX-42 immunoreactive microglial cells at 5 days PS are distributed randomly throughout the tissue. Both putative parenchymal (solid arrows) and perivascular (solid arrowhead) microglia are apparent. B. OX-1 microglial staining pattern at 5 days PS demonstrates a similar pattern to, but a higher staining intensity than, OX-42 labeled cells (solid arrows). C. NGFR immunoreactive microglia are located predominately surrounding and extending out from blood vessels as long velate projections (solid arrows). Magnification, 650X.

The NGFR staining pattern showed similarities as well as some differences compared to OX-42 and OX-1 staining patterns in the distribution of the NGFR-IR cells. Distinctly labeled microglial cells appear to be located within the NL parenchyma. However, the majority of the NGFR-immunoreactive sites have a more reticular and somewhat velate appearance. This is particularly evident surrounding the blood vessels and the 192-IgG positive cells appear to be localized primarily within the perivascular space. This staining pattern becomes more evident with time and is particularly well illustrated at 90 days PS. The OX-42 and OX-1 staining patterns show no maturational change.

#### Morphometric Assessment of Glial Cell Numbers

Astrocyte hypertrophy and proliferation have been reported to occur both within and surrounding sites of brain injury in a variety of experimental paradigms (Sjostrand, 1966; Rose et al., 1976; Latov et al., 1979; Nathaniel and Nathaniel, 1981). Perivascular and parenchymal microglia have also been implicated in the extensive gliosis which accompanies brain injury (Streit and Kreutzberg, 1988; Streit et al., 1989). We too have reported an injury-related increase in the area of the NL occupied by glial elements which reached peak levels by five days post-surgery before gradually returning to normal a month later (Watt and Paden, 1991). However, the specific glial cell populations contributing were not determined. Therefore an investigation was undertaken to determine whether glial proliferation and/or cellular hypertrophy might account for the observed increase in glial area.

The initial experiment involved determining the relative density of pituicyte and microglial cells by counting glial nuclei in one micron coronal sections of toluidine blue stained plastic-embedded NL at varying times following knife cut (Table 2). As illustrated in Figure 20, a significant increase ( $F=10.7$ ,  $P<.0001$ , one way ANOVA,  $df=9/23$ ) in pituicyte nuclear density was observed within 48 hours of denervation

which then remained above normal for 30 continuous days. By 2 days PS, pituicyte nuclei have increased a significant 39% above intact control values ( $P < .05$ , Neuman-Keuls). This increase was reduced slightly by 5 days PS reaching a value of 36% above normal ( $P < .05$ , Neuman-Keuls). The pituicyte numbers continue to decrease with no significant difference observed between PS 30 lesion animals and controls.

Table 2. Results of Glial Cell Counts - Lesion Group Means\*.

Exp. Group	Pituicytes	Microglia	NL Area mm <sup>2</sup>	Pits/mm <sup>2</sup>	Micro/mm <sup>2</sup>
Lesion Animals:					
2 dps	418.0 ± 11.5	293.0 ± 18.2	.34	1229.4 ± 49.1	861.8 ± 38.0
5 dps	309.0 ± 26.1	225.0 ± 24.9	.26	1188.0 ± 39.2	865.4 ± 130.4
10 dps	395.0 ± 21.2	257.1 ± 18.0	.37	1067.5 ± 17.1	694.8 ± 13.0
30 dps	239.7 ± 23.8	179.4 ± 8.9	.26	921.9 ± 68.4	690.0 ± 40.9
90 dps	91.6 ± 18.4	93.25 ± 16.2	.12	763.2 ± 54.5	777.1 ± 57.3
150 dps	197.3 ± 15.7	125.2 ± 6.7	.39	505.7 ± 32.3	321.0 ± 46.0
Intact Control Animals:					
0 dps	315.0 ± 23.7	293.0 ± 34.9	.37	851.3 ± 69.2	800.8 ± 36.1
10 dps	210.0 ± 12.9	154.2 ± 9.5	.23	913.4 ± 46.2	669.0 ± 37.8
30 dps	190.2 ± 13.6	121.6 ± 14.5	.26	731.6 ± 67.3	467.5 ± 43.4
90 dps	102.7 ± 8.8	91.7 ± 12.6	.41	250.4 ± 46.1	764.0 ± 47.3

Four animals were included in all lesion groups.

Three coronal sections were analyzed per animal.

Three animals were included in all control groups except 0 dps which included four.

\*Mean ± sem

Days post-surgery (dps) or equivalent age for sham controls.

We have previously reported shrinkage of the NL at 10 days following surgery with a return to normal size by 30 days PS (Watt and Paden, 1991). Such a reduction in NL cross-sectional area would almost certainly result in an apparent increase of cell density in the absence of glial death. However, the substantial elevation in pituicyte nuclei observed at 30 days PS provides strong evidence that the increase in cell density noted here reflects a true increase in relative pituicyte cell numbers.

Further analysis of pituicyte contribution to the observed gliosis was investigated by measuring the cross-sectional area of pituicyte













































































